Tectonic development of the western branch of the East African rift system

C. J. EBINGER* *Massachusetts Institute of Technology/Woods Hole Oceanographic Institution Joint Program, Department of Earth, Atmospheric, & Planetary Sciences, Massachusetts Institute of Technology, Cambridge, Massachusetts 02139*

ABSTRACT

The Western rift, the western branch of the East African rift system, is bordered by high-angle normal fault systems bounding one side of spoon-shaped basins. Depth-to-detachment estimates of 20–30 km, the rollover geometry of asymmetric basins, and seismicity throughout the depth range 0–30 km suggest that planar border faults along one side of rift basins penetrate the crust. Along the length of the rift, ~100-km-long *en echelon* border-fault segments are linked by oblique-slip transfer faults, ramps, and monoclines within comparatively high-strain accommodation zones. These transfer faults accommodate significant along-axis variations in the elevation of basins and uplifted rift flanks but do not appear to extend outside the 40- to 70-km-wide rift basins across the uplifted flanks. Kinematic constraints from several basins indicate a regional east-west extension direction that is consistent with existing seismicity data. Estimates of crustal extension based on fault geometries interpreted from seismic reflection data and field observations within 13 basins are less than 15% (<10 km). Volcanism began at ~12 Ma in the north and at ~7 Ma in the south prior to or concurrent with the initial development of Western rift sedimentary basins. During Pleistocene time, asymmetric basins have narrowed through progressive hanging-wall collapse and with uplift of the rift flanks. These geometric and temporal patterns of development are similar to those of the more magmatically active Kenya rift, where volcanic activity began ~11 m.y. prior to initial volcanism in the Western rift. Both the poor correlation between Miocene–Recent border and transfer faults and pre-Miocene shear zones, and the repetitive basin geometries indicate that the along-axis segmentation generally is not inherited. Western rift border-fault segments propagated to the north and south to link originally isolated basins, and this along-axis propagation contributes to the segmentation of the Western rift valley.

INTRODUCTION

The volcanically and seismically active East African rift system lies atop a broad intracontinental swell, the East African Plateau, and consists of two branches, the Western and Kenya (Gregory) rift valleys (Fig. 1). In earlier tectonic models of the East African rift system, both the Kenya and Western rift systems have been interpreted as incipient plate boundaries linked to the Afar–Red Sea–Gulf of Aden rift systems to the northeast (for example, Gregory, 1896; Fairhead and Girdler, 1969; Degens and others, 1971; McConnell, 1972; Chorowicz, 1983; Courtillot and others, 1987). No connection between the two approximately north-south–striking Western and Kenya rifts, however, is apparent in structural, morphologic, or seismicity patterns. Tectonic interpretations differ in the timing, direction, and amount of crustal extension within the East African rift system, largely owing to lack of observational constraints within the Western rift (for example, Fairhead and Girdler, 1969; Chorowicz, 1983; Shudofsky, 1985; Rosendahl and others, 1986; Ebinger and others, 1987; Morley, 1988a; Tiercelin and others, 1988).

Seismic, gravity, and bathymetric data from the Western and Kenya rifts show that the two rift valleys are segmented along their length into a series of generally asymmetric basins approximately 100 km in length (for example, King, 1978; Crossley and Crow, 1980; Chorowicz, 1983; Ebinger and others, 1984; Bosworth, 1985; Rosendahl and others, 1986; Baker, 1986; Morley, 1988a). The three-dimensional geometry and continuity of Tertiary faults bounding and linking Western rift basins and the extent of faulting across the broad uplifted rift flanks, however, were poorly understood prior to this study (Fig. 1b). Earlier compilations of East African rift structures commonly have included inactive structures shown by recent studies to be pre-Tertiary in age, and considerable variations in age of volcanic sequences within and between the Kenya and Western rift valleys have been reported (for example, Baker and others, 1971; Bellon and Pouclet, 1980; Crossley and Knight, 1981; Tiercelin and others, 1988). In order to estimate crustal extension and to evaluate tectonic models of the East African rift system, a detailed chronology of subsidence, rift flank uplift, and volcanism along the length of the lesser known Western rift is needed. When evaluated on a basin-by-basin basis, spatial and temporal relations repeated along the length of the Western rift provide constraints on the nature and cause of the along-axis segmentation of this active continental rift.

The objectives of this study are (1) to use consistent structural and stratigraphic criteria to delineate individual extensional basins along the length of the Western rift, (2) to summarize geometric and kinematic constraints on the timing and amount of vertical and horizontal crustal movements within the Western rift system, and (3) to use these structural and stratigraphic observations to evaluate mechanisms for the along-axis segmentation of the rift. The results of this regional synthesis are compared to interpretations of the better-known Kenya rift located along the eastern side of the East African Plateau. Detailed field observations within several representative rift basins supplement structural interpretations of 30-m–resolution Landsat imagery, reports, and geologic maps and extend interpretations of seismic reflection profiles from Western rift lake basins across the uplifted rift flanks. Field studies in the Western rift also were designed to enhance and check existing structural and stratigraphic interpretations, and to obtain kinematic constraints on the timing and direction of extension.

*Present address: Geodynamics Branch, National Aeronautics and Space Administration/Goddard Space Flight Center, Greenbelt, Maryland 20771.

Geological Society of America Bulletin, v. 101, p. 885–903, 14 figs., 2 tables, July 1989.

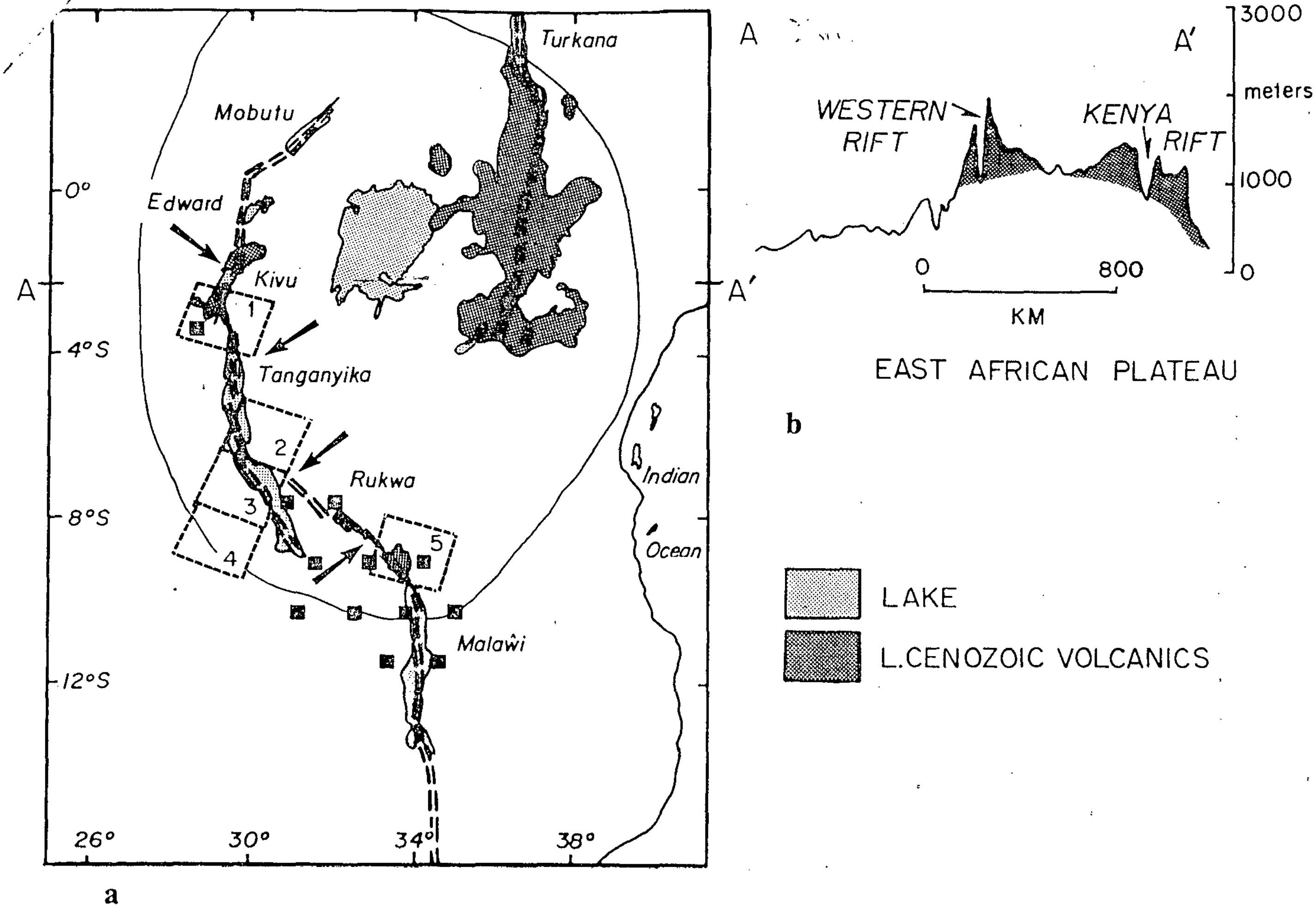

Figure 1. a. Tertiary volcanic provinces of East African rift system; lakes filling parts of the Western rift valley labeled. Boxes show coverage provided by high-resolution Thematic Mapper (5) and Multi-Spectral Scanner (MSS) (1–4) images; small squares show approximate centers of black-and-white MSS imagery used in analyses. Arrows point to regions outside scenes 1–5 where field studies were conducted. Elevations greater than 800 m within uplifted East African Plateau enclosed by light line. Dashed double line shows the approximate position of the Western and Kenya rift valley floors. b. Topographic profile A–A′ across East African Plateau. Shading emphasizes approximately 400-km-wide zone of uplift flanking rift valleys.

BACKGROUND

Geophysical evidence for crustal thinning across the 1,300-km-wide East African Plateau is restricted to 40- to 75-km-wide zones beneath the Western and Kenya rift valleys (Rykounov and others, 1972; Bram and Schmeling, 1975; Maguire and Long, 1976; Hebert and Langston, 1985; KRISP, 1987). On the basis of seismic refraction data, crustal thinning beneath the northern part of the Western rift system is less than 25%; crustal thickness estimates from the Edward-Kivu rift systems and the Kivu-Tanganyika rifts are approximately 30 km, or 5–11 km less than those found beneath the East African Plateau outside the rift valleys (Bram and Schmeling, 1975; Maguire and Long, 1976; Hebert and Langston, 1985). Because refraction profiles average crustal structure over distances of 200–800 km, however, crustal thickness beneath individual rift basins may be less. If an approximately east-west extension direction is assumed, estimates of crustal thinning based on reconstructions of surface fault geometries in the Tanganyika rift range from 2%–15%, and isostatic models of subsidence patterns within the Malawi rift indicate that the crust has been thinned by less than 25% (Ebinger and others, 1987, 1989; Morley, 1988a). Along the length of the Western rift system, numerous small-magnitude earthquakes generally with tensional focal mechanisms occur throughout the depth range 0–30 km with no apparent vertical gap in seismicity (Wohlenberg, 1968; Rodrigues, 1970; Zana and Hamaguchi, 1978; Brown and Girdler, 1980; Fairhead and Stuart, 1982; Shudofsky, 1985). Recent analyses of gravity data from East Africa suggest that thermal processes and faulting have weakened the lithosphere beneath the Western rift valley relative to that beneath the uplifted craton (Ebinger and others, 1989).

The earliest volcanism in the East African Plateau region occurred at 23 Ma in the central plateau region and near the future site of the Kenya rift system (for example, Baker and others, 1971) (Table 1). Initial uplift of at least the eastern part of the plateau began in early Miocene time, and sediments shed from the uplifted plateau were deposited rapidly within the marine basin along the Indian Ocean margin of Africa (Saggerson and Baker, 1965; Shackleton, 1978; King, 1978; Coffin and Rabinowitz, 1983). Although Paleogene ^{40}K-^{40}Ar ages have been reported (for example, Bellon and Pouclet,

TABLE 1. CHRONOLOGIC CONSTRAINTS FROM EAST AFRICAN DOME REGION, USED IN FIGURE 14

Site	Description	Age (m.y.)	Reference
A	Samburu basalts, K/Ar	23.0 ± 0.2	Baker and others, 1971
B	Mount Elgon nephelinite, K/Ar	22.0 ± 0.2*	Baker and others, 1971
C	Rusinga Island tuff, K/Ar	17.9 ± 0.1	Drake and others, 1988
D	Kishalduga nephelinite, K/Ar	15.1	Crossley and Knight, 1981
E	Elgeyo phonolite, K/Ar	13.6 ± 0.6	Crossley and Knight, 1981
F	Kapiti phonolite, K/Ar	13.1 ± 0.5	Crossley and Knight, 1981
G	Virunga alkali basalt, K/Ar	12.6 ± 0.7	Bellon and Pouclet, 1980
H	S. Kivu tholeiite, K/Ar	10.0 ± 0.6	Pasteels and others, 1989
I	S. Kivu alkali basalt, K/Ar	8.5 ± 0.5	Pasteels and others, 1989
J	Mobutu basin, fauna	~8	M. Pickford, 1989, personal commun.
K	Rungwe phonolite, K/Ar	7.2 ± 0.6	Ebinger and others, 1989
L	Ol Esayeiti trachyte, K/Ar	6.7	Baker and others, 1971
M	Rusizi basin sediments, fauna	~5.0	D. Stone, 1987, personal commun.
N	Chiwondo beds, fauna	4–5	Kaufulu and others, 1981
O	Mount Sodiman nephelinite, K/Ar	4.5 ± 0.4	Bagdasaryan and others, 1973
P	Edward basin sediments, fauna†	4.1	P. Williamson, 1987, personal commun.
Q	Ngorongoro basalt, K/Ar	3.7 ± 0.8	P. Williamson, 1987, personal commun.
R	Mount Kenya syenite, K/Ar	3.1	Baker and others, 1971
S	Usangu (Mbeya) picrite, K/Ar	3.04 ± 0.04	Ebinger and others, 1989
T	Kilimanjaro nephelinite, K/Ar	2.3 ± 0.4	Bagdasaryan and others, 1973
U	Songwe trachyte, K/Ar	0.55 ± 0.01	Ebinger and others, 1989
V	Toro-Ankole mafurite, K/Ar	0.45 ± 0.15	Bagdasaryan and others, 1973

*Faunal evidence suggests that Mount Elgon basalts are approximately 18 m.y. old (M. Pickford, 1989, personal commun.).
†Base of section not seen.

1980; Kampunzu and others, 1983; Tiercelin and others, 1988), recent radiometric analyses of volcanic rocks indicate that initial volcanism within the Western rift commenced at approximately 12 Ma in the north, and volcanic activity continues to historic times within the isolated Western rift volcanic provinces (Harkin, 1960; Bagdasaryan and others, 1973; Bellon and Pouclet, 1980; Pasteels and others, 1989; Ebinger and others, 1989). Mid-Miocene–age fauna found in fluvial sequences of the Mobutu (Albert) basin and an extrapolation of Holocene sedimentation rates have been cited as evidence for initial faulting during early Miocene time (Hopwood and Lepersonne, 1953; Patterson, 1983). In the southern part of the Western rift system, the oldest reported lacustrine sediments contain fossils dated at 6–5 Ma (Kaufulu and others, 1981; C. Morley, 1988, personal commun.).

The East African rift system formed largely within Proterozoic orogenic belts surrounding the Archean cratons of central and eastern Africa, although faults bounding the central rift fracture unmetamorphosed cratonic rocks (Fig. 2). In a regional sense, the location of the two rift valleys follows Proterozoic orogenic belts and avoids the central craton, possibly reflecting pre-existing heterogeneity in lithospheric strength across the 1,300-km-wide plateau (for example, McConnell, 1972). Metamorphic basement beneath the Western rift is characterized by northwest-trending, northeast-trending, and approximately north-south–trending mylonites and shear zones (for example, Reeves, 1960; Cahen and Snelling, 1984; Theunissen, 1986; Daly, 1986; Klerkx and Nanyaro, 1988) (Fig. 2). Within parts of the East African rift system, upper Paleozoic–Mesozoic sedimentary sequences deposited in rift basins underlie Tertiary sequences (for example, Arambourg, 1933; Spence, 1954; Dixey, 1956; Williamson and Savage, 1986).

WESTERN RIFT BASINS

Approximately 100-km-long normal fault systems with 1- to 6-km throws bound the deeper side of asymmetric basins (border-fault segments), and the sense of basinal asymmetry commonly alternates along the length of the rift valley (Crossley and Crow, 1980; Ebinger and others, 1984; Rosendahl and others, 1986; Peirce and Lipkov, 1988; Burgess and others, 1989). The broad flanks of the Western rift have been uplifted 1–4 km above the surrounding topography of the East African Plateau, and metamorphic basement lies below sea level beneath many basins (for example, Figs. 1b, 3). Although basin linkage by ductile deformation within accommodation zones has been suggested, *en echelon* border-fault segments are connected by oblique-slip transfer faults and relay ramps in parts of East Africa (for example, King, 1978; Bosworth, 1985; Rosendahl and others, 1986; Ebinger, 1989). Existing geologic maps from the Western rift region, however, are at a scale of 1:2,000,000, and more detailed geologic reports generally have focused on mineral resources and ~~Precambrian~~ structures. Thus, late Cenozoic structures were unreported or undifferentiated from Precambrian and Mesozoic structures in much of the Western rift.

Field studies and enhanced color Landsat-5 Thematic Mapper (TM) and Multi-Spectral Scanner (MSS) imagery supplemented by 1:50,000 aerial photographs were used as a primary data base to examine fault patterns between discrete rift basins and along the uplifted flanks of the Western rift valley and to integrate existing maps from the region (see App. 1; Fig. 1). Transects of 14 rift flanks along ~east-west continuations of Project PROBE seismic reflection profiles of lake basins and detailed studies in 5 rift basins were made in 1986 and 1987. In order to extend these structural interpretations between the specific field study locales shown in Figure 1, a mosaic of 1:1,000,000 MSS imagery provided by Musée Royale de l'Afrique Centrale was assembled. Where faults and lineaments had not been noted previously, the following criteria were used to differentiate Neogene faults from older structures in imagery: amount of topographic relief, appearance of fault scarps, occurrence of hot springs, and horizontal offsets of pre-rift basement faults and geologic contacts. The scale of topographic maps used in the field and to interpret Landsat imagery was generally 1:50,000.

Sediment thickness, fault geometries, and the sense of asymmetry within rift basins are derived from interpretations of single-channel and multichannel seismic reflection data, aeromagnetic data, and gravity data from Lake Tanganyika (Degens and others, 1971; Patterson, 1983; Lorber, 1984; Rosendahl and others, 1986; Burgess and others, 1989), Lake Kivu (Degens and others, 1973), the Rusizi basin (D. Stone, 1987, personal commun.), the Rukwa rift (Peirce and Lipkov, 1988; C. Morley, 1988, personal commun.), and the Malawi rift (Ebinger and others, 1987). Seismicity patterns and depth to detachment estimates (for example, Gibbs, 1983) provide information on border-fault geometries at depth.

Generalized Three-Dimensional Geometry of Western Basins

Structural relations within the Moba and Marungu basins of Lake Tanganyika illustrate the

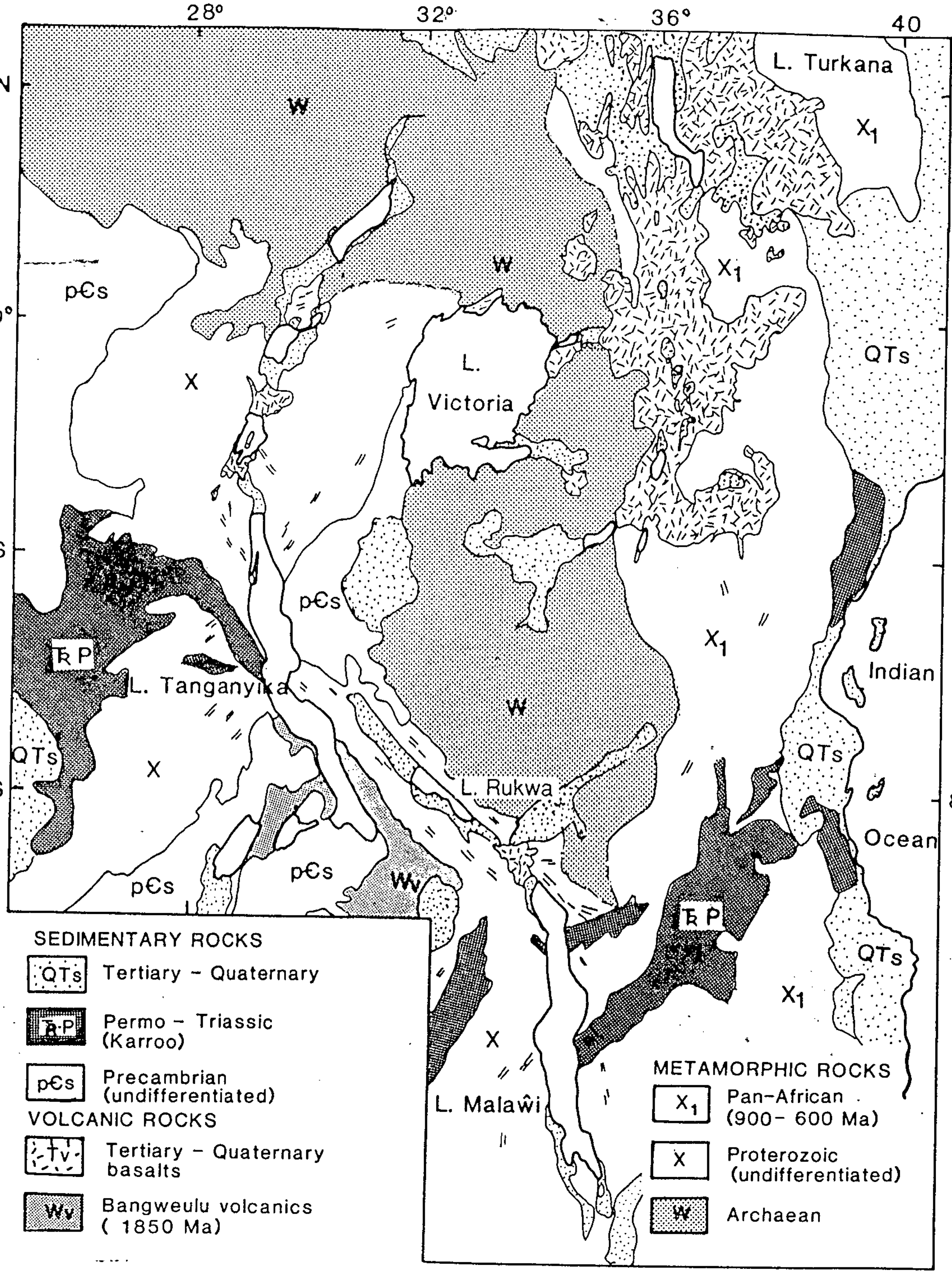

Figure 2. Summary of East African geology, emphasizing Permian-Triassic rift basins (dark shading). Regional structural trends within Precambrian orogenic belts indicated by short lines. Note that several Western rift basins have developed within Archean basement. Geologic information from Afonso (1976), Baker (1986), Cahen and Snelling (1984), Carter and Bennett (1973), Kent and others (1971), Lepersonne (1977), Quennell and others (1956), Reeves (1960).

typical three-dimensional geometry of Western rift border faults and basins. On the basis of the distinct asymmetry in topographic and bathymetric relief and sediment thickness variations apparent in seismic reflection data, I interpret two border segments along the southwestern margin of Lake Tanganyika (Rosendahl and others, 1986) (Fig. 4). High-angle (45°–75°) normal faults with throws of 100 m or more occur in a 10- to 15-km-wide zone along the western margins of the Moba and Marungu basins, and these faults are characterized by triangular scarps in Landsat scene 3 and aerial photographs (Fig. 5). Faults bounding the Moba basin strike northwest; those bounding the Ma-

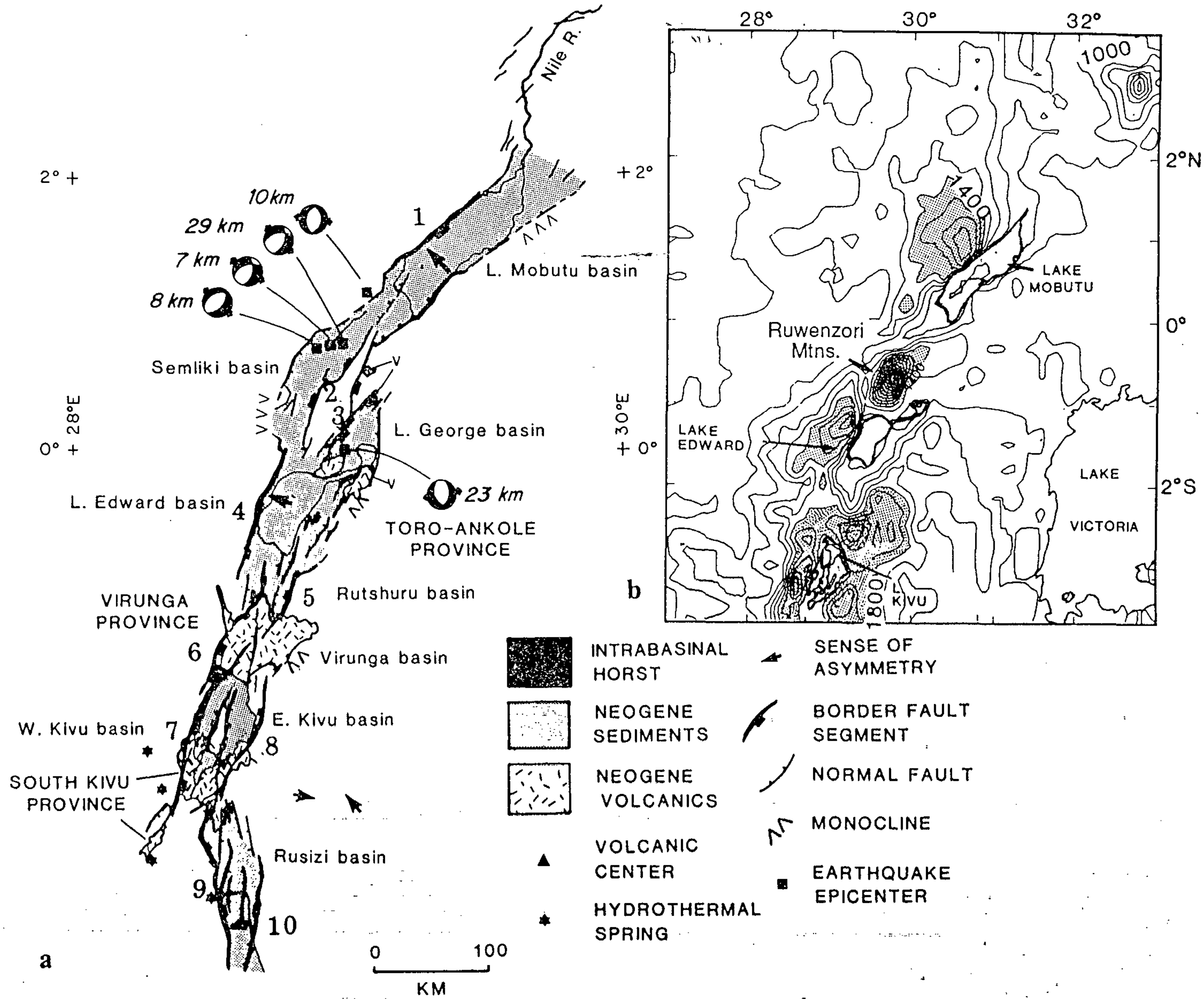

Figure 3. a. Tectonic interpretation of rift basins bounded by border-fault segments (BFS's) 1–10 described in text. Focal mechanism solutions of earthquakes with epicentral locations denoted by squares shown as lower-hemisphere projections; hypocentral depths as indicated (from Shudofsky, 1985). Sense of basin asymmetry indicated where known. Structural interpretations from Holmes (1951), Davies (1951), Pouclet (1977), Degens and others (1973), this study. b. Smoothed contours of topographic relief, showing rift valley topography and regional elevation variations. Contour interval, 200 m; elevations above 1,400 m (Albert-Edward) and 1,800 m (Kivu) shown shaded to illustrate asymmetry of rift flank uplift.

rungu basin strike approximately north-south (Figs. 5, 6). Northwest-striking faults interpreted as oblique-slip faults commonly exhibit subhorizontal slickenside striations (Figs. 5, 6) (Chorowicz, 1983). The geometrical arrangement of generally linear faults along these ~100-km-long border-fault segments produces a curvilinear basin margin (Fig. 6).

The approximately 2,000-m-high plateau on the western side of the Moba and Marungu basins dips gently to the west away from the rift valley, and no evidence for faulting is found outside the inner-facing normal faults (Figs. 5, 6, and 7). The eastern margins of both basins are structural monoclines, and metamorphic basement dips gently to the west beneath sedimentary sequences contained in these two basins (Fig. 7). Thus, sedimentary basins bounded by these 10- to 15-km-wide systems of high-angle normal faults (border-fault segments) have the characteristic cross-sectional form of half-graben (Fig. 7). Seismic velocity control, however, is inadequate to place tight constraints on the geometry of border faults at depth (for example, Rosendahl and others, 1986).

The Moba basin is characterized by 5- to 10-km-wide tilted blocks that generally trend northwest parallel to normal faults bounding the Moba basin. Faults within the Marungu basin generally strike north-south parallel to Marungu border faults (Fig. 6). Synsedimentary faults penetrate to all stratigraphic levels of the sedimentary sequence within both basins, although

Figure 4. a. Tectonic interpretation of rift basins bounded by border-fault segments (BFS's) 11–23 described in text. Focal mechanism solutions of earthquakes with epicentral locations denoted by squares shown as lower-hemisphere projections; hypocentral depths as indicated (from Shudofsky, 1985). Structural patterns from Harkin (1960), Chorowicz (1983), Rosendahl and others (1986), Ebinger and others (1987), Peirce and Lipkov (1988), this study. b. Topographic relief along central part of Western rift valley. Contour interval, 200 m; elevations above 1,400 m shown shaded. Basinal regions indicated by line pattern.

a

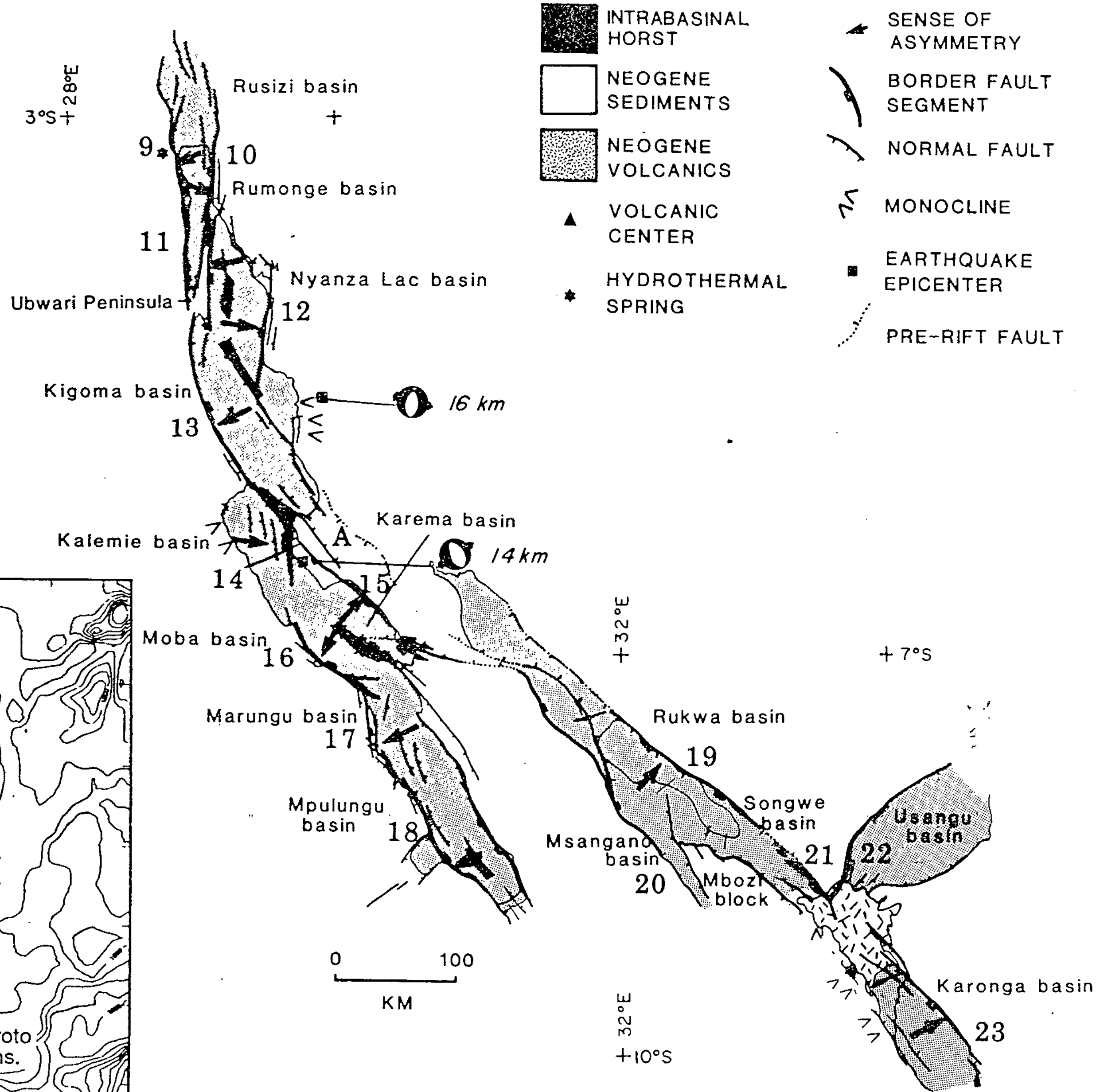

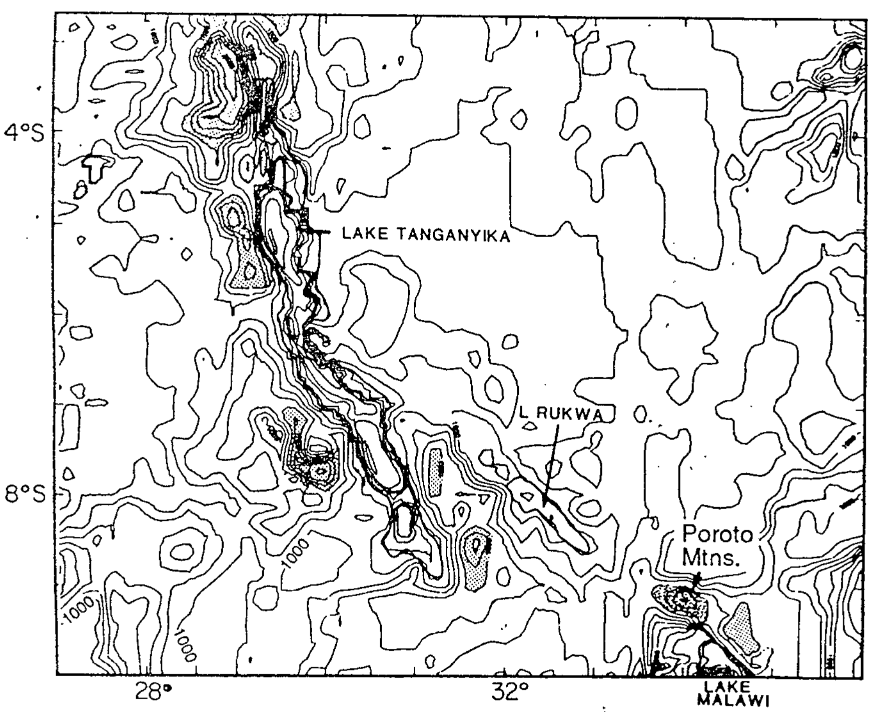

b

the magnitude of subsidence is greater in the Marungu basin than in the Moba basin (Morley, 1988a) (Fig. 7; Table 2). Sedimentary accumulations are greatest near the central part of border-fault segments and decrease toward the tips, producing spoon-shaped basin morphologies (Figs. 6, 7). Estimates of extension based on the geometry of faults offsetting metamorphic and/or acoustic basement are 4–5 km (~10%), or slightly more than the 3 km estimated by Morley (1988a) based on seismic data alone (Table 2). On the basis of balanced cross sections, depth to detachment for faults bounding these basins is ~25 km.

Dip-slip and oblique-slip transfer faults bounding the western margin of Lake Tanganyika intersect at the tips of the two border-fault segments, an interbasinal accommodation zone (Figs. 5, 6, and 8). Within the accommodation zone, a basement ridge separates the two basins, but seismic coverage is insufficient to constrain the geometry of faults linking the two extensional basins beneath the lake (for example, Rosendahl and others, 1986; Morley, 1988a). On the eastern side of the rift, normal faults strike N20°W and N10°E (Fig. 8b). Subhorizontal slickenside striations indicate that the most recent displacement along east-west-striking faults was strike slip, but no lithologic or structural indicators were found to document the sense and amount of offset (Figs. 8b, 9).

Faults bounding the Moba and Marungu basins cut unmetamorphosed and homogeneous Archean and Precambrian basement and, therefore, should be unaffected by pre-existing crustal weaknesses (Figs. 2, 6). The northern part of the Moba border-fault segment extends across a fault contact between lower Proterozoic and Archean rocks with no change in fault orientation (Z, Fig. 6). Faults on the eastern side of the basins are oblique to metamorphic foliations and mylonites striking N60°W (Fig. 8b).

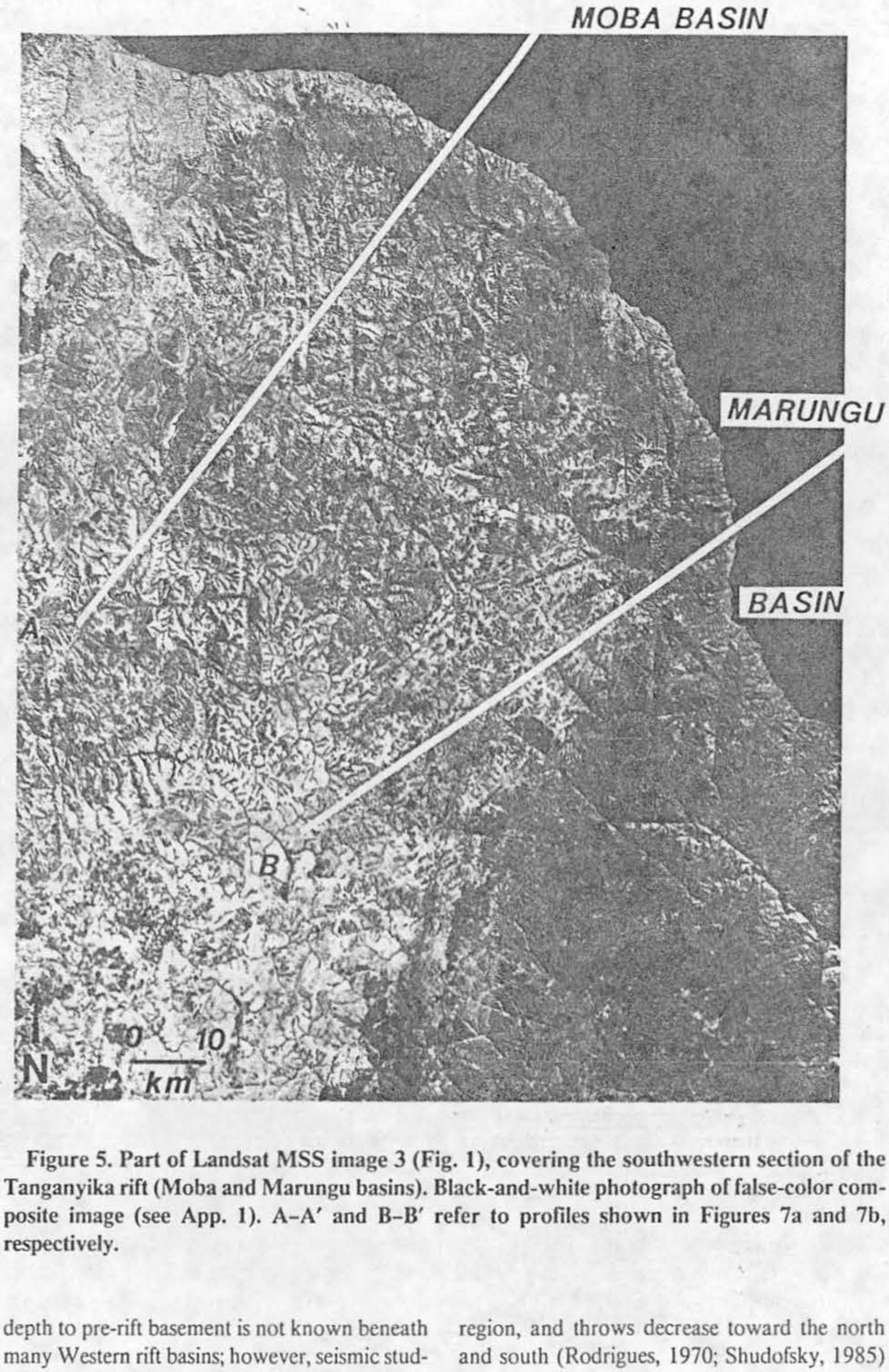

Figure 5. Part of Landsat MSS image 3 (Fig. 1), covering the southwestern section of the Tanganyika rift (Moba and Marungu basins). Black-and-white photograph of false-color composite image (see App. 1). A–A′ and B–B′ refer to profiles shown in Figures 7a and 7b, respectively.

Basinal Descriptions

Regional tectonic maps of rift basins bounded by border-fault segments (BFS's) 1–23 shown in Figures 3 and 4 and briefly described from north to south are based on similar analyses of topography, surface and subsurface structures, and analogy to border-fault geometries illustrated above. New and existing constraints on crustal extension, border-fault geometries, and the timing of subsidence, uplift, and volcanism are described briefly and in Table 2. Accommodation zones are identified, but the variable geometry of transfer faults within specific accommodation zones requires more detailed analyses (for example, King, 1978; Ebinger, 1989). For comparative purposes, maximum amounts of subsidence within basins are listed as present elevations of the rift valley or lake floor because depth to pre-rift basement is not known beneath many Western rift basins; however, seismic studies within Western rift lake basins show that depth to pre-rift basement generally follows bathymetric contours (for example, Degens and others, 1971; Wong and Von Herzen, 1974; Ebinger and others, 1984; Rosendahl and others, 1986).

Mobutu Basin (BFS1)

The northwestern margin of the Mobutu (Albert) basin is bounded by BFS1 (Fig. 3a). At its central part, the seismically active Mobutu escarpment rises 1,300 m above the surrounding region, and throws decrease toward the north and south (Rodrigues, 1970; Shudofsky, 1985) (Fig. 3b). Hot salt-water springs and oil seeps have been reported along the base of the Mobutu escarpment (Davies, 1951). The fault-plane mechanism determined by Shudofsky (1985) for an earthquake at 10 km depth beneath the Mobutu basin indicates pure normal faulting along a north-south–striking fault plane (Fig. 3a). On the eastern side of the basin, the eastward-tilted surface of westward-dipping faults form a stair-step pattern (step faults) rising to the elevation of the uplifted East African Plateau (Davies, 1951). Borehole data indicate that at least 1,250 m of fluvio-lacustrine sedimentary

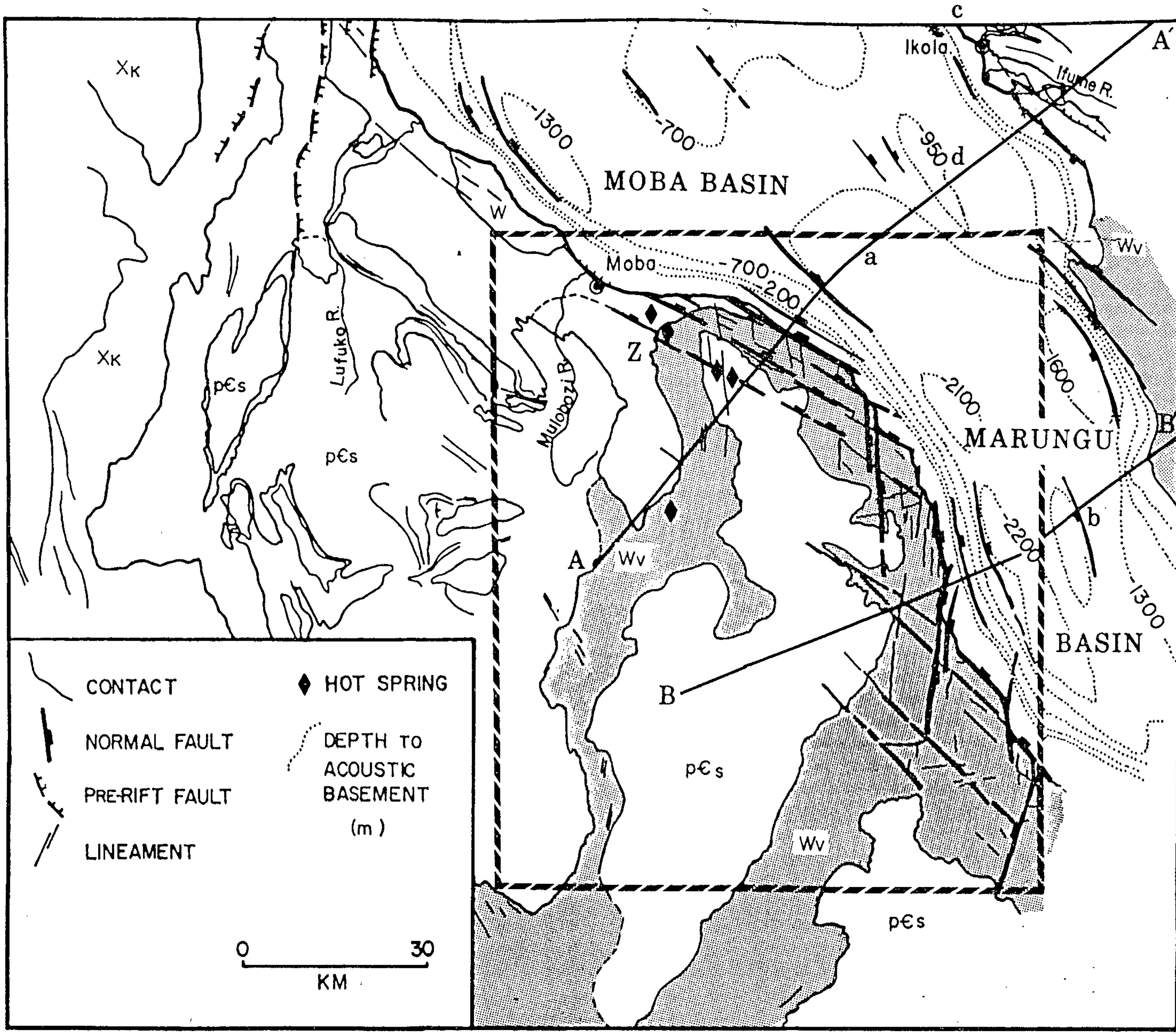

Figure 6. Interpretation of lineaments observed in part of MSS image 3. Faults have formed in undeformed Archean volcanic sequence (Wv); flat-lying sedimentary rocks (p€s) along the uplifted flank roughly correspond to highest elevations. Geologic legend same as in Figure 2; Xκ, Kibaran belt (Late Proterozoic). Z denotes structural contact referred to in text. Box encloses region shown in Figure 5; fault patterns in upper right corner shown in Figure 8b. A–a–A′, B–b–B′ refer to cross-sectional profiles shown in Figures 7a and 7b, respectively. Location of hydrothermal springs from Tshimanga and Kabengele (1981); lithologic units and basement structures from Lepersonne (1977) and McConnell (1950). Depths to basement corrected for sediment loading calculated from sediment isopach maps shown in Burgess and others (1989) and using sediment loading correction described in Crough (1983).

sequences have accumulated within the Mobutu basin (Davies, 1951). Early Miocene fauna within basal fluvial sequences have been reported, but the earliest lacustrine sequences were dated at ~8 Ma (Hopwood and Lepersonne, 1953; Pickford, 1989, personal commun.).

Semliki Basin (BFS2)

The Semliki basin is bounded by a series of normal faults dipping N60°–80°W along the western side of the 5,200-m-high Ruwenzori mountains, and a faulted monocline bounds the northwestern margin of the Semliki basin (Fig. 3). Fault planes inferred from focal mechanisms of earthquakes that occurred at depths of 7–29 km beneath the Semliki basin strike N20°E, or parallel to the strike of normal faults bounding the Semliki basin (Shudofsky, 1985; Fig. 3a). At the northern end of the Semliki basin, Pliocene-Pleistocene units correlative with those found in the Mobutu basin crop out along the nose formed by the intersection of the monocline and BFS2 (Wayland, 1934; Holmes, 1951). Numerous hot springs are found along the escarpment, and hanging valleys and sediment terraces attest to Holocene faulting within the Semliki basin (Davies, 1951).

Lake George Basin (BFS3)

Faults with large throws and triangular scarps bound the eastern margin of the Ruwenzori

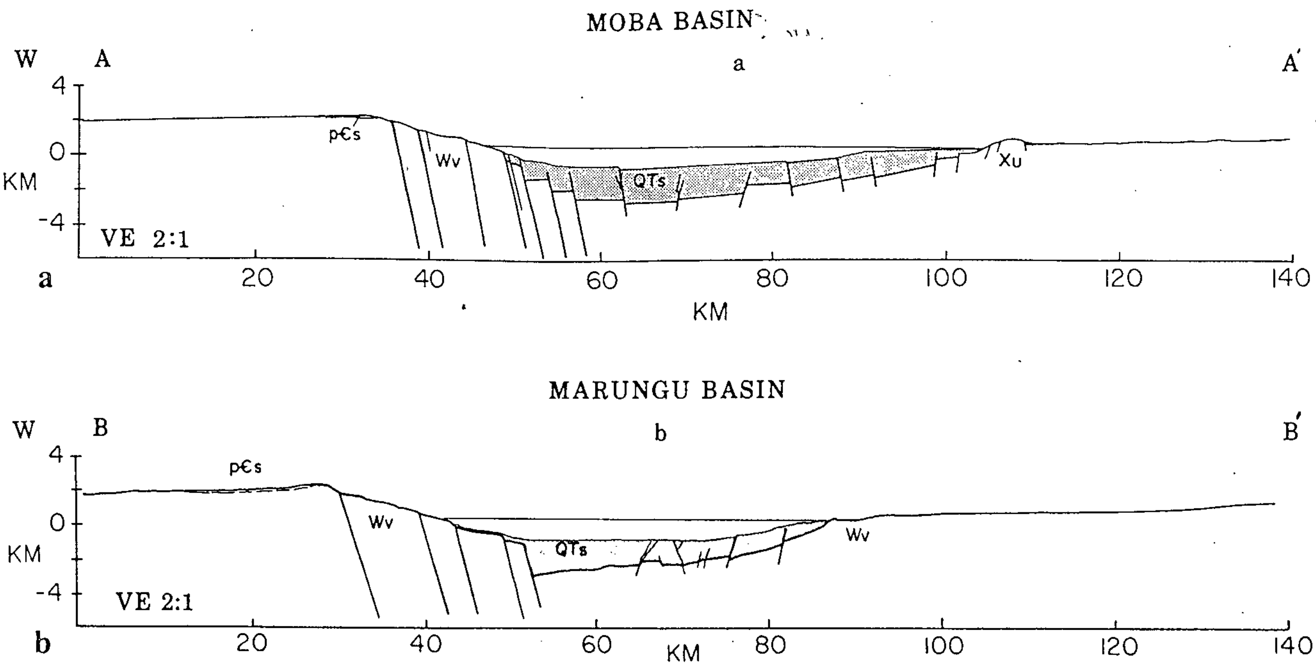

Figure 7. Cross-sectional profiles of Moba and Marungu basins vertically exaggerated (VE = 2:1) to illustrate uplifted flanks and basinal morphology. a. Cross-sectional profile of Moba basin along line A-a-A' (Figs. 5 and 6). Cross-sectional profile of Marungu basin along line B-b-B' (Figs. 5 and 6). Structural patterns beneath lake from interpretation of seismic profiles 90 and 220, respectively (after Rosendahl and others, 1986).

TABLE 2. SUMMARY OF BORDER-FAULT GEOMETRIES, SENSE AND MAGNITUDE OF ASYMMETRY WITHIN BASINS (?, PREDICTED), CRUSTAL EXTENSION (IN KILOMETERS), DEPTH TO DETACHMENT (DD), AND CHRONOLOGIC CONSTRAINTS FROM WESTERN RIFT BASINS

Border-fault segment	Basin	Strike/ asymmetry	Extension/ DD (km)	Flank(m)/ subsidence (m)	Age (m.y.)	Reference
1	Mobutu	N30°E/NW		2,500/570	~8	(a)
2	Semliki	N20°E/SE?		5,200/760	<4.1	(b)
3	L. George	N20°E/NW?		5,200/760		
Toro-Ankole volcanic province					<1	(c)
4	L. Edward	N10°E/NW		3,090/900		
5	Rutshuru	N10°E/SE?		2,080/1,120	Qs terraces	(d)
6	Virunga	N10°E/NW?		2,500/1,100	Qs terraces	(d)
Virunga volcanic province					12.6	(e)
7	West Kivu	N20°E/NW	<3/~23	3,300/960	<8.5	
8	East Kivu	N20°E/SE	<3/~23	2,950/1,060	<10; Qs terraces	
South Kivu volcanic province					10.0	(g)
9	Rusizi	N10°W/SW	1*-2.5/20	3,300/400	<5; Qs terraces	(h)
10	Rumonge	N-S/E	2.5	2,600/250		
11	W. Nyanza-lac	N-S/W	3*-3.5/~20	1,620/-250		
12	E. Nyanza-lac	N-S/E	~2*	1,920/-480		
13	Kigoma	N20°W/SW	4*-6/20	2,750/-540		
14	Kalemie	N-S/E	3.5*-5/22	2,460/-120		
15	East Moba	N30°W/NE		1,940/20		
16	West Moba	N30°W/SW	3*-5	2,340/0		
17	Marungu	N-S/W	3*-4/25	2,430/-630		
18	Mpulungu	N20°W/W	~3*	2,200/20		
19	Rukwa	N30°W/NE		1,691/790	<6	(h)
20	Msangano	N20°W/W?		2,200/900		
21	Songwe	N30°W/NE		2,820/900	<1	(f)
Rungwe volcanic province					7.2	(f)
22	Usangu	N20°E/NW?		2,300/950	<3	(f)
23	Karonga	N30°W/NE	~3/~20	2,930/-800	<5	(f,i)
24	W. Nkhata Bay	N-S/W		2,360/-165		
25	E. Nkhata Bay	N-S/E		1,980/200		
26	Likoma	N20°E/NW	<5	1,930/110		
27	N. Nkhotakota	N-S/W		1,820/150		
28	S. Nkhotakota	N-S/E		1,820/200		
29	E. Monkey Bay	N10°W/NE?		1,825/370		
30	W. Monkey Bay	N10°W/NE?		2,180/370		
31	Shire	N25°E/SE		2,070/470		
32	Urema	N40°W/NE		1,445/68		

Note: elevation of rift flanks and basins referenced to sea level; maximum subsidence within basins listed as elevation of the rift valley or lake floor because depth to pre-rift basement is not known in many basins. Maximum sediment thickness beneath Tanganyika lake basins in Rosendahl and others (1986), Morley (1988a); Lake Kivu, in Wong and Von Herzen (1974); and Lake Malawi, in Ebinger and others (1987). Qs terraces indicates Quaternary lake sequences found along uplifted basin margins.

(a) M. Pickford (1989, personal commun.)
(b) P. Williamson (1987, personal commun.)
(c) Bagdasaryan and others (1973)
(d) Pouclet (1975)
(e) Bellon and Pouclet (1980)
(f) Ebinger and others (1989)
(g) Pasteels and others (1989)
(h) C. Morley (1988, personal commun.)
(i) Kaufulu and others (1981)

*Indicates extension estimate from Morley (1988a).

mountains (BFS3; Fig. 3a). On the basis of the focal mechanism from an earthquake at approximately 29 km depth beneath the eastern margin of the basin (Shudofsky, 1985), the extension direction is approximately perpendicular to the strike of BFS3 (Fig. 3a). Subdued topographic relief along the eastern margin suggests that the Lake George basin is tilted to the west, and the basin contains Pliocene-Pleistocene sedimentary sequences (Wayland, 1934) (Fig. 3b). Pleistocene alkali basalts of the Toro-Ankole province are found along the northern part of BFS3, and isolated vents and craters mark the margins of tilted fault blocks within the accommodation zone between BFS3 and BFS4 (Fig. 3a) (Combe, 1943; Bagdasaryan and others, 1973).

Lake Edward Basin (BFS4)

Relay ramps (for example, King, 1978) link the northwestern side of the Semliki basin with BFS4. Throws along BFS4 are greatest near the north-central part of Lake Edward, and a northwestward tilt is inferred from bathymetry (Fig. 3a). High-angle *en echelon* normal faults with minor throws border the southeastern side of the Edward basin (Hopwood, 1970). Faunal remains within the lacustrine Kaiso beds have been correlated to Pliocene stratigraphic sequences in the northern part of the Kenya rift system (Table 2). Periods of basinal desiccation correlated with major faunal radiations at 4 Ma and between 2 and 3 Ma may be related to episodes of faulting and uplift along BFS4 (P. Williamson, 1987, personal commun.).

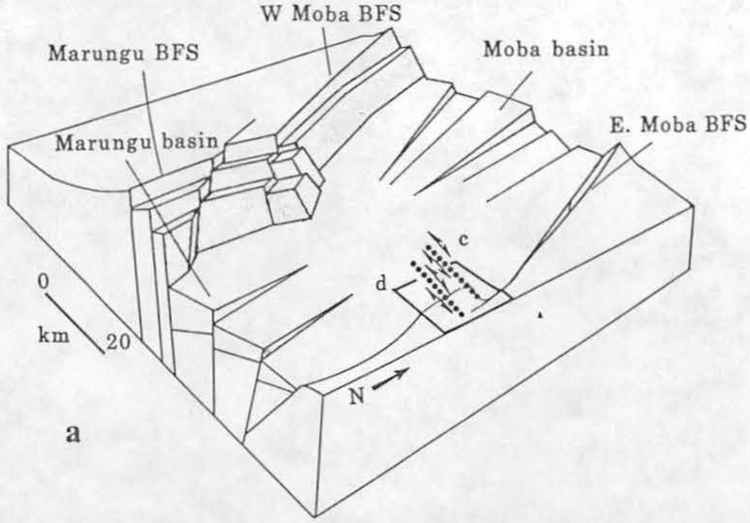

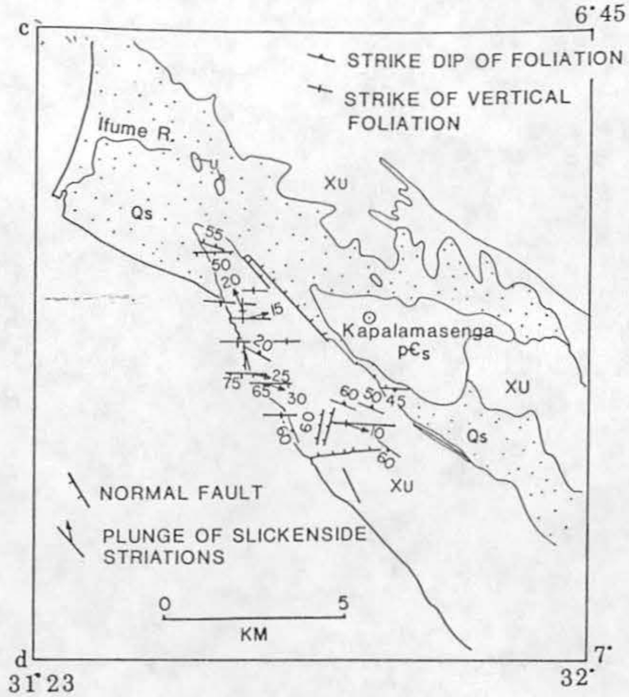

Figure 8. a. Schematic diagram of border-fault segments and morphology of Moba and Marungu basins. Intersection of Moba (N30°W strike) and Marungu (north-south strike) border-fault systems produces zig-zag lake outline (for example, Fig. 5). Strike-slip faults (dotted lines) interpreted from fault patterns in region shown in Figure 8b. b. Late Cenozoic faults and metamorphic foliations along eastern margin of Moba basin. Fault surfaces oriented approximately east-west commonly show subhorizontal slickenside striations. Note gneissic foliation (N30°–40°W) oblique to normal and strike-slip faults. Legend same as in Figure 2. Xu, Ubendian belt; Qs, Quaternary sedimentary rocks.

Figure 9. Slickenside striations plunge 15° to N80°E along surface of fault striking N85°E along eastern margin of Moba basin (see Fig. 6). Foliation of augen gneisses N35°W/40°SW.

Rutshuru Basin (BFS5)

The eastward-tilted Rutshuru basin is bounded by a north-south-striking border-fault segment (BFS5; Fig. 3b). Basalts from the Virunga province to the south cover lake sedimentary sequences that crop out along terraces found at 1,225, 1,300, 1,400, 1,450, and 1,600 m above the Rutshuru valley floor and at least 500 m above the highest reported lake level (de la Vallée Poussin, 1933; Pouclet, 1977).

Virunga Basin (BFS6)

High-angle (50°–70°) east-dipping faults border the western margin of the Virunga basin (Fig. 3b) (Pouclet, 1977). Within the accommodation zone between the Virunga basin and the Kivu basin, northwest-striking fissures marked by active shield volcanoes crosscut the rift valley (Fig. 3). The spatial distribution of basalt flows within the Virunga basin suggests that initial volcanism at 12.6 Ma preceded or was concurrent with initial faulting and basinal subsidence (Bellon and Pouclet, 1980). Along the length of BFS6, step faults are capped by

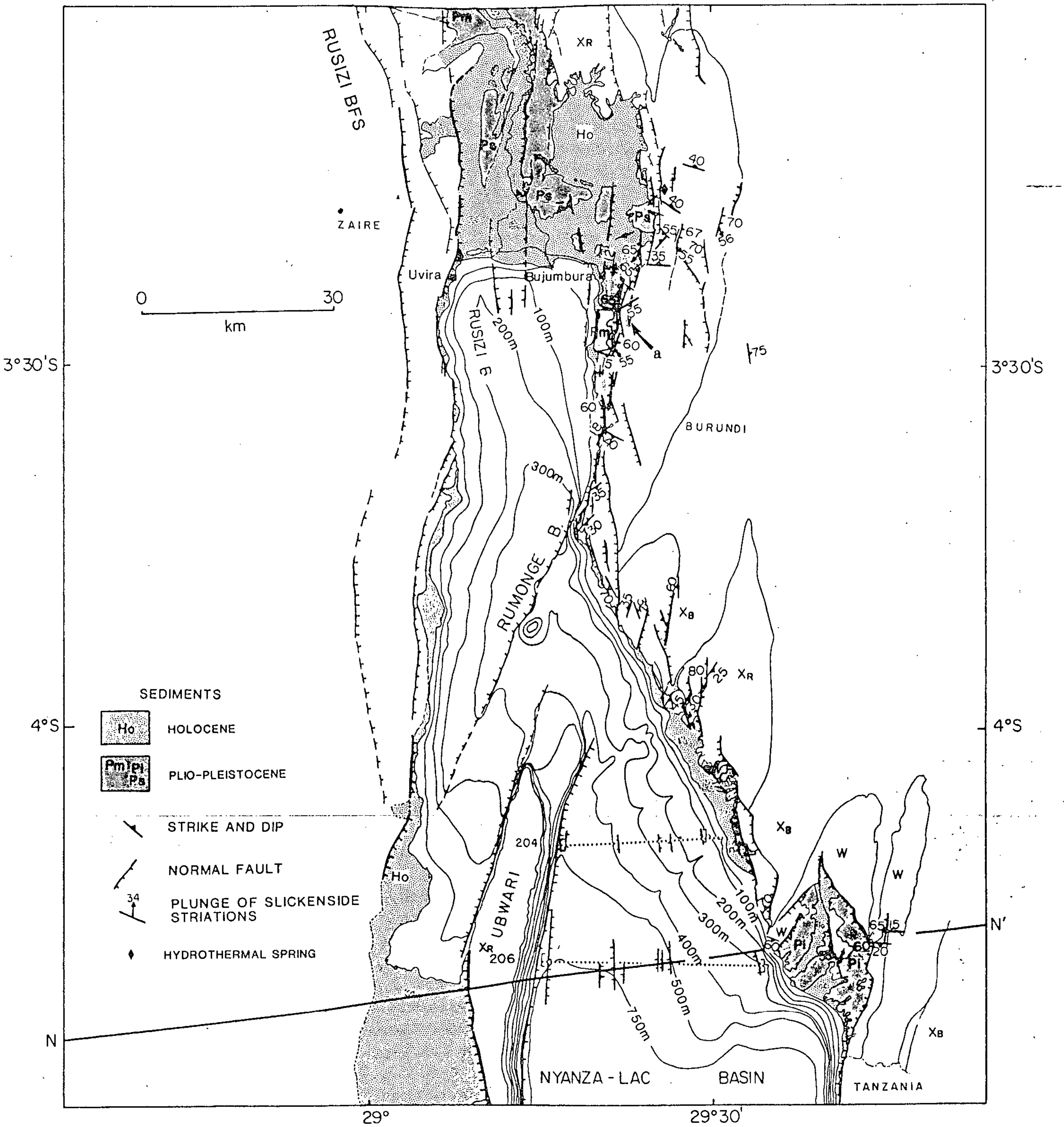

Figure 10. Fault patterns along the northern part of the Tanganyika rift; bathymetric contours beneath Lake Tanganyika in meters below lake level (774 m). Fault patterns based on field mapping and interpretation of aerial photographs. Lithologic contacts and basement structures from Lepersonne (1977), Theunissen (1986, 1989a, 1989b), Ilunga (1984). Structural information beneath Lake Tanganyika from multi-channel seismic reflection profiles 204 and 206 (dotted lines) provided by B. Rosendahl (1986, personal commun.); single-channel data from Patterson (1983). Bold line N–N′ indicates location of cross section shown in Figure 11. W, Archean; X_R, Rusizian; X_B, Burundian.

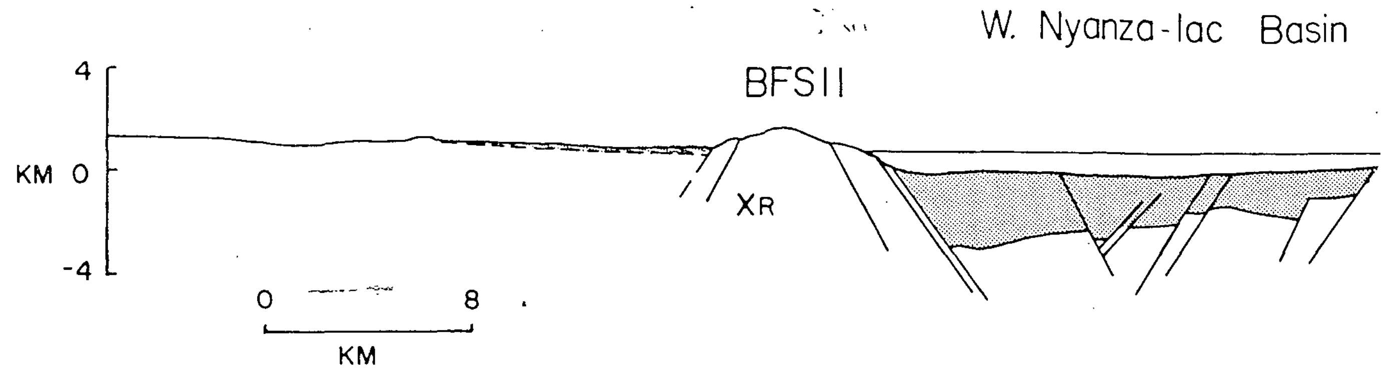

Figure 11. Geologic cross section of the Nyanza-lac basin including the northern part of the Nyanza-lac border-fault segment that crosscuts Archean basement (N–N′; Fig. 10). Dashed lines are Precambrian thrust faults (from Theunissen, 1986). Estimate of crustal extension, <15%; depth to detachment, 20–25 km. Note rollover geometry of basin, with zone of maximum subsidence near the base of BFS11. (Note slight overlap in center.)

terraces of Pliocene-Pleistocene lacustrine sequences at elevations of 1,450, 1,500, 1,650, 2,000, and 2,050 m, and the highest terrace is now 800 m above the Quaternary lake level highstand (Pouclet, 1975). Holocene basalts from Karisimbi volcano have been uplifted on the monoclinal side of the basin (Pouclet, 1975; De Mulder and Pasteels, 1986). This rift flank uplift effectively narrowed the zone of subsidence within the Virunga basin.

Kivu Basins (BFS7, BFS8)

The western side of Lake Kivu is bounded by BFS7, and the West Kivu basin is filled with as much as 500 m of sedimentary units and basalts from the Virunga province (Fig. 3b; Wong and Von Herzen, 1974). Quaternary cinder cones aligned along the central section of this escarpment are located within the inner-facing normal faults bounding the rift valley (Guibert, 1977; Bellon and Pouclet, 1980; Ebinger, 1989). A second border-fault segment, BFS8, bounds the East Kivu basin (Fig. 3a). In this geometrical arrangement, a horst serves as a hinge for subsidence along both BFS7 and BFS8 (Fig. 3a). If plane strain and extension normal to border faults are assumed, estimates of crustal extension based on surface fault geometries measured along a cross section of the Kivu rift are less than 10 km (<15%), and depth to detachment is 23 km or more (Table 2).

Tholeiitic volcanism along the East Kivu border-fault segment began in mid-Miocene time, and alkalic volcanism within the West Kivu and East Kivu basins began in late Miocene time (Table 1). Tholeiitic and alkalic basalts were erupted along both margins of the Kivu rift and the horst in Quaternary time (Pasteels and others, 1989; Ebinger, 1989). Field observations and seismicity patterns indicate that the West Kivu border-fault segment has served as the master fault for crustal extension during Quaternary time (Ebinger, 1989). Uplift along the central part of BFS8 elevated a terrace of late Pleistocene lacustrine sequences ~500 m above the lake level highstand (Ebinger, 1989).

Rusizi Basin (BFS9)

The Rusizi border-fault segment follows the western margin of the westward-tilted Rusizi basin (Figs. 4, 10). Earthquake epicenters during the period 1958–1965 within the Rusizi basin cluster along the central Rusizi border-fault segment, and epicentral depths throughout the range 0–30 km have been reported within the Rusizi basin (Wohlenberg, 1968; Zana and Hamaguchi, 1978). The eastern side of the Rusizi basin is bounded by faceted step faults that dip 60°–75° to the west (Fig. 10). Slickenside striations along border faults and transfer faults indicate an approximately east-west extension direction, with ~2 km extension measured across the basin and flanks (Ebinger, 1989).

Upper Miocene–Pleistocene lacustrine sequences are interbedded with and/or overlie basalts dated at 6.5–5 Ma that have been correlated with sequences within the Kivu basins (Tack and DePaepe, 1983; Ilunga, 1984; Chorowicz and Thouin, 1985; Pasteels and others, 1989; Ebinger, 1989). Sequences thicken to more than 1,500 m in the central part of the basin beneath Lake Tanganyika, with metamorphic basement lying nearly 1,200 m lower than basement beneath the Kivu basins (Patterson, 1983; Morley, 1988a; Ebinger, 1989). This elevation difference is accommodated by east-northeast–striking oblique-slip faults linking the East Kivu and Rusizi border-fault segments. Faults bounding the northwestern Rusizi basin formed during late Miocene time and propagated northward during Pliocene-Pleistocene time. Terraces of lacustrine sedimentary sequences found in thin lenses between eastward-tilted fault blocks are elevated nearly 500 m above Lake Tanganyika (location a, Fig. 10; Table 1).

Rumonge Basin (BFS10)

The sense of asymmetry within the Rumonge basin is down-to-the-east, opposite to the sense of asymmetry within the Rusizi basin (Figs. 4a, 10). The southern tip of the Rumonge border-fault segment extends beneath Lake Tanganyika where normal faults striking N10°E continue to the southwest of the Ubwari peninsula (Fig. 10). As along the Kivu fault systems, there is no evidence for Neogene faults along the uplifted flanks outside the rift valley where topographic relief is gentle (Fig. 4b).

Nyanza-lac Basins (BFS11, BFS12)

The eastern side of the Ubwari peninsula is bounded by a border-fault segment defining a narrow westward-tilted basin (Figs. 10, 11; Rosendahl and others, 1986; Morley, 1988a). An intrabasinal horst separates the West Nyanza-lac basin bounded by BFS11 from the East Nyanza-lac basin bounded by BFS12, a half-graben tilted to the east. Thus, the cross-sectional morphology of the rift valley is similar to that of the Kivu basin (Fig. 4). The rift flank outside BFS12 dips gently to the east with no evidence for recent faulting outside inner-facing faults bordering the rift valley (Figs. 11, 12). On the basis of fault geometries shown in Figure 11 and if one assumes plane strain, crustal extension

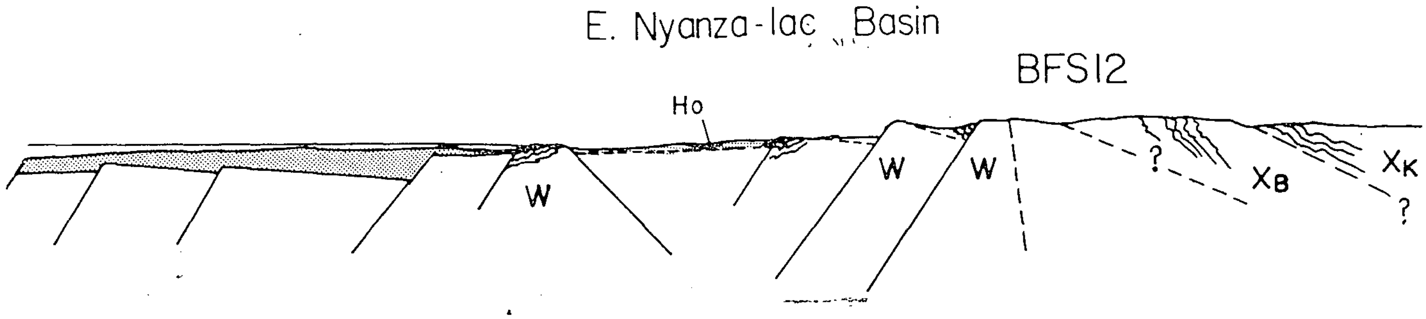

Figure 11. (*Continued*).

is less than 4 km (15%), or slightly more than an earlier estimate of 3 km based on seismic data alone (Morley, 1988a). Balanced cross-section estimates indicate that the depth to detachment for faults within the Nyanza-lac basin is 20 km or more (for example, Morley, 1988a) (Table 2).

Kigoma Basin (BFS13)

A shallow northwest-striking ridge separates the Nyanza-lac basin from the westward-tilted Kigoma basin (Fig. 4b; Table 2). More than 4 km of sedimentary rocks has accumulated at the base of this steep escarpment (Rosendahl and others, 1986). The southern end of the Kigoma basin border-fault segment curves to the east and bounds a shallow ridge in the accommodation zone between the Kigoma and Kalemie basins (Fig. 4a).

Kalemie Basin (BFS14)

North-south–striking faults with triangular scarps bound the eastern side of the Kalemie basin (Fig. 4, Table 2). Northwest-striking faults bounding a horst separating the Kigoma and Kalemie basins have been interpreted as strike-slip faults (Lorber, 1984). Tilted fault blocks within the Kalemie basin trend north-south (Rosendahl and others, 1986; Burgess and others, 1989). BFS13 continues to the south along the eastern flank of BFS14 outside the rift valley (Fig. 4a).

Karema Basin (BFS15)

An earthquake at 12 km depth with a southwest-northeast tensional axis (Shudofsky, 1985), or perpendicular to the northwest strike of BFS15, occurred beneath the eastern Karema basin (Fig. 4a). Faults within the Karema basin may reactivate Permian-Triassic normal faults in the accommodation zone between the Kalemie and Karema basins (Fig. 4a). The Karema basin is separated from the Moba basin by a horst (for example, Rosendahl and others, 1986; Morley, 1988a).

Moba Basin (BFS16), Marungu Basin (BFS17)

Significant throw during Quaternary time along the Marungu border-fault segment is indicated by V-shaped river valleys that are found at greater than 500 m water depth at the base of the Marungu BFS (Capart, 1949).

Mpulungu Basin (BFS18)

Fault systems bounding the Western rift valley splay at the southern end of the Mpulungu basin where throws decrease to less than 1 km (Chorowicz, 1983; Rosendahl and others, 1986; Morley, 1988a). Along the eastern flank of the Mpulungu basin, a mid-Miocene erosional surface has been uplifted relative to the East African Plateau to the east, and Pleistocene lacustrine sequences 300 m above Lake Tanganyika attest to Quaternary uplift (Grantham and others, 1958; Haldemann, 1969).

Rukwa Basin (BFS19)

Recent exploratory studies indicate that at least 5 km of sediment has accumulated at the base of BFS19 (Spence, 1954; Brown, 1964; Peirce and Lipkov, 1988; C. Morley, 1988, personal commun.). In contrast to other strongly asymmetric Western rift basins (for example, Kigoma basin), the flank of BFS19 rises less than 400 m above the East African Plateau, and the western (monoclinal) side of the rift is nearly 1,000 m higher (Table 2; Fig. 4b). Along the eastern side of the Rukwa basin, normal faults that cut Holocene lacustrine sequences of the Rukwa trough have a N0°–20°W strike that is oblique to N45°W-striking normal faults bounding the eastern side of the Rukwa trough (Fick and Van der Heyde, 1959; Peirce and Lipkov, 1988; this study). On the basis of exploratory drilling (Amoco Production Company), clastic sequences within the Rukwa basin previously assigned to Late Cretaceous time now have been shown to be late Miocene (Table 2) (Spence, 1954; Tiercelin and others, 1988; C. Morley, 1988, personal commun.).

Msangano Basin (BFS20)

Late Cenozoic faults bound the western margin of the narrow Msangano basin (BFS20), where < 100 m of sedimentary sequence overlies metamorphic basement (Peirce and Lipkov, 1988; Tiercelin and others, 1988). Normal fault scarps largely are uneroded and triangular, in comparison to the deeply dissected fault system bounding the eastern margin of the Msangano basin. Lacustrine sedimentary sequences compositionally similar to Pleistocene sequences found at higher elevations within the Rukwa trough and within the adjacent Songwe basin indicate that faulting occurred after mid-Pleistocene time (Brock, 1962; Ebinger and others, 1989).

Songwe Basin (BFS21)

The narrow Songwe basin is bounded on its northwestern side by a series of high-angle (60°–80°) step faults, commonly with subvertical slickenside striations (Grantham and others, 1958; Ebinger and others, 1989). Dip-slip and oblique-slip faults become more numerous and fault-block rotations increase from less than 10° to 30° near the comparatively high-strain accommodation zone between the Songwe and Karonga basins (Ebinger and others, 1989). Within the accommodation zone, fissures and cinder cones mark *en echelon* eastward-tilted faults of BFS21 (Ebinger and others, 1989). An elongate Jurassic-Cretaceous carbonatite body

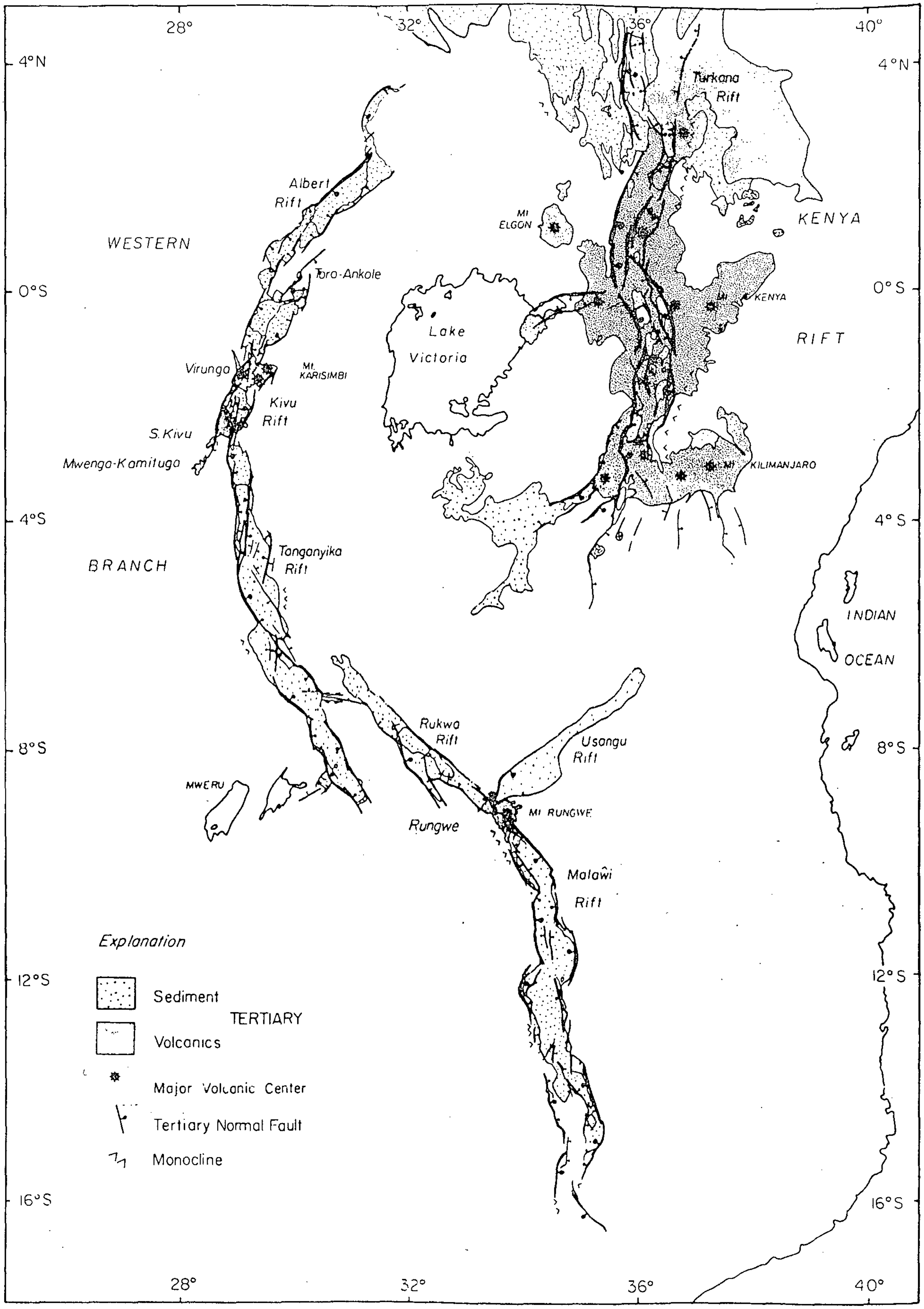

Figure 12. Major structures of the Tertiary East African rift system, summarized from Figures 3 and 4. Structural interpretation of Kenya rift from Baker (1986) and Bosworth (1985).

has been exhumed by recent faulting, suggesting that the Songwe border-fault segment has reactivated a pre-rift shear zone (Fick and Van der Heyde, 1959; Brown, 1964). Pleistocene-Recent volcanic flows from eruptive centers within the Songwe basin are interbedded with and overlie ~200 m of volcaniclastic lake units and Cretaceous (?) sequences (Grantham and others, 1958; Ebinger and others, 1989).

Usangu Basin (BFS22)

The Usangu basin is bounded by a system of north-south-striking step faults rising to the level of the uplifted Usangu flank (Fig. 4). The faulted southeastern margin of the Usangu basin is the uplifted flank of the Karonga basin to the south (Fig. 4a). Field observations and gravity data from the Usangu basin indicate that a <1-km sequence of basalt flows and volcaniclastic units overlies metamorphic basement within the Usangu basin. Pliocene-Recent volcaniclastic sequences tilted ~10° have accumulated along the downthrown sides of 1- to 5-km-wide tilted blocks bounded by N30°–40°E–striking normal faults (Teale and others, 1962; this study). As in other parts of the Western rift, eruptive volcanic centers coincide with closely spaced faults within the high-strain accommodation zone between the Usangu and Karonga basins (Ebinger and others, 1989). The Usangu border-fault segment developed in early Pliocene time, or after initial volcanism within the Rungwe province (Ebinger and others, 1989).

Karonga Basin (BFS23)

Throws along BFS23 are greatest near the central part of the Karonga basin where the rift valley is filled by Lake Malawi, and I find little evidence for late Cenozoic faulting along the uplifted flanks (Fig. 4). The opposite side of the Karonga basin is bordered by a regional monocline of dissected Mesozoic sequences and metamorphic basement (Stockley, 1948; Harkin and Harpum, 1978; Crossley and Crow, 1980). Cinder cones commonly mark east-northeast–striking oblique-slip transfer faults connecting BFS23 and BFS21, and slickenside striations within the accommodation zone suggest an approximately east-northeast extension direction (Ebinger and others, 1989). If plane strain is assumed, late Cenozoic crustal extension is 2.7–3.5 km (5%–9%), and depth to detachment estimated from a balanced cross section is 20 km or more. Late Miocene volcanic centers displaced by border faults indicate that BFS23 developed after 7.2 Ma (Table 1) (Ebinger and others, 1989). Alkali basalt flows dated at ~5 Ma derived from centers along intrabasinal faults were erupted at about the same time as the oldest known sedimentary sequences in the Karonga basin (Kaufulu and others, 1981; Ebinger and others, 1989). Upper Pleistocene basalt flows have been offset 50–70 m in the past 0.10 m.y., or, extrapolating 2.5–3.5 km in the past 5 m.y. (Ebinger and others, 1989).

Malawi (Nyasa) Rift Basins

The Malawi rift continues to the south of the uplifted East African Plateau and consists of nine border-fault segments (excluding BFS23) that have been delineated using these same criteria (Ebinger and others, 1987; Table 2). Throws along Malawi rift border-fault segments vary from more than 4 km in the Karonga and Nkhata Bay basins to less than 1 km in the Shire basin at the southern end of the Malawi rift. Seismic stratigraphic sequences vary between basins and only the uppermost sequence occurs lake-wide, suggesting that rift segments have developed diachronously (Ebinger and others, 1984). No constraints on the age of basal sedimentary sequences are available from the Malawi rift, however.

EXTENSIONAL BASIN GEOMETRY

The discontinuous Western rift, including the Malawi rift, comprises at least 32 basins bounded by approximately 100-km-long systems of dip-slip and oblique-slip faults (border-fault segments; Fig. 12). The flanks of the rift outside basins are uplifted 1–4 km above the elevation of the East African Plateau, and the magnitude of uplift is generally greater along the side of the basin bounded by the border-fault segment (for example, Figs. 3, 4, 7, and 11). Along the length of the rift, depth to pre-rift basement beneath basins varies by several kilometers in part owing to the regional uplift of the East African Plateau (Table 2; Rosendahl and others, 1986). If the topographic relief of the rift is partly or wholly flexurally compensated, these elevation differences may be due to varying amounts of crustal extension and the geometrical arrangement of border faults that effectively fracture the elastic lithosphere beneath the rifts (for example, Weissel and others, 1987; Ebinger and others, 1989).

Contours of poles to planes of border-fault segments 1–32 (surface dips) and earthquake focal mechanisms show the average north-south strike of border faults (Fig. 13a). Both earthquake focal mechanisms and slips interpreted from slickenside striations within Western rift basins support an east-west extension direction (Fig. 13b). Balanced cross sections and fault geometries within 13 lake basins and their faulted margins indicate that the crust beneath Western rift basins has been thinned by less than 15% (<10 km), assuming plane strain and an approximately east-west extension direction. These estimates are slightly more than those based on interpretations of seismic reflection profiles alone (Morley, 1988a; see Table 2). Depth-to-detachment calculations within several rift basins indicate that normal faults extend to depths greater than 20 km (for example, Fig. 11; Morley, 1988a). If deformation internal to fault blocks is common, these estimates of crustal extension and depth to detachment represent minimum estimates. The rollover geometry characteristic of Western rift basins (for example, Fig. 11) is consistent with planar normal faults that extend to lower crustal levels (for example, Gibbs, 1984).

On the basis of detailed field studies supplemented by geophysical data, *en echelon* border-fault segments are linked by relay ramps and transfer faults within comparatively high-strain accommodation zones. Roughly comparable amounts of extension (2–10 km) and throws (1–6 km) along border-fault segments lead to a

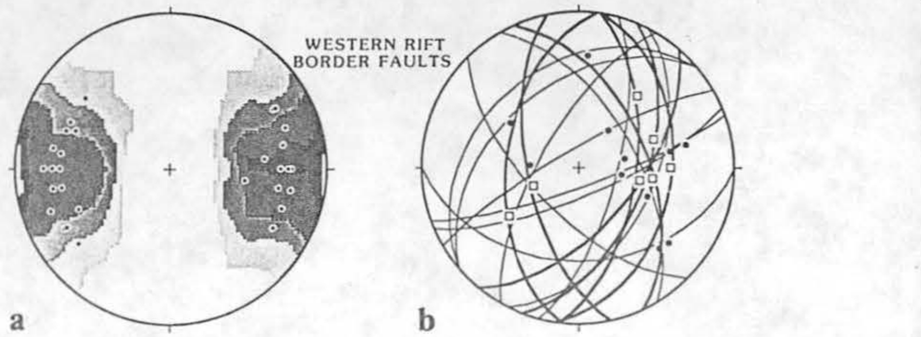

Figure 13. Equal-area lower-hemisphere projections. a. Contours of poles to fault planes of border-fault segments listed in Table 2 (surface dips plotted) and earthquake focal planes listed in Shudofsky (1985). Contour interval, 2σ. b. Slip vectors and planes of slickenside striations (light lines) within the Western rift (bold dots). Slips along focal planes (bold lines) were converted to plunge (open squares) (after Shudofsky, 1985).

predominance of oblique-slip transfer faults, in contrast to strike-slip faults linking shallow crustal detachments in other continental rifts (for example, Burchfiel and Stewart, 1966; Gibbs, 1983, 1984). Because Western rift transfer faults accommodate large differences in elevation between adjoining basins and their uplifted flanks, as well as regional variations in topographic relief related to the 1,300-km-wide East African Plateau, half-graben commonly are separated along the length of the rift valley by horsts or sills (for example, Kivu/Rusizi accommodation zone).

The location of volcanic provinces and volcanic centers within these provinces shows several consistent correlations with rift basin development. In a regional sense, the Toro-Ankole, Virunga, South Kivu, and Rungwe volcanic provinces coincide with interbasinal accommodation zones (Figs. 3, 4; Table 2). Eruptive centers within Western rift volcanic provinces are restricted to rift basins within the inner-facing normal faults, although in some instances, basalts from centers located along border faults have flowed down outward-tilted flanks away from the rift (for example, Usangu basin). Within these volcanic provinces, chains of volcanic centers are aligned along the tips of border-fault segments and along oblique-slip transfer faults crosscutting the rift valley (for example, Pouclet, 1975; Ebinger and others, 1989). The general occurrence of volcanic centers along the tips of border-fault segments and along oblique-slip faults linking basins reflects the higher density of faults within accommodation zones. This coincidence also suggests that transfer faults are steeper at lower crustal levels than are the central parts of border-fault segments.

Three structural relations consistently observed along the length of the Western rift valley strongly suggest that zones of crustal thinning are limited to rift basins and that the crust beneath the rift flanks is unthinned. First, few faults occur on the uplifted flanks outside inner-facing normal faults bounding the rift valley. Second, detailed field studies in four accommodation zones indicate that oblique-slip faults linking basins do not extend outside the rift valley across the rift flanks. Third, the absence of volcanic centers along the rift flanks reflects a lack of faulting along the rift flanks.

In mechanical models proposed to explain alternating basinal asymmetries, it is assumed that border-fault segments serve as detachments for crustal and/or lithospheric extension; differences among the models are related to the geometry of the detachment faults and their along-axis linkage (for example, Bally, 1982; Gibbs, 1984; Wernicke, 1985; Mohr, 1987; Bosworth, 1987). In order to explain alternating basin asymmetries in the East African rift system, Bosworth (1987) and Mohr (1987) suggested that sub-crustal lithospheric-scale detachments beneath the rift flanks are linked by ~300-km-wide accommodation zones. There is, however, no evidence for extension or continuation of transfer faults outside 40- to 70-km-wide Western rift basins. Likewise, spatial patterns of uplift and volcanism predicted by thermo-mechanical models of asymmetric lithospheric detachments are in poor agreement with observations in the Western rift (for example, Buck and others, 1988). Instead, earthquake epicentral depths throughout the range of 0–30 km, the deep

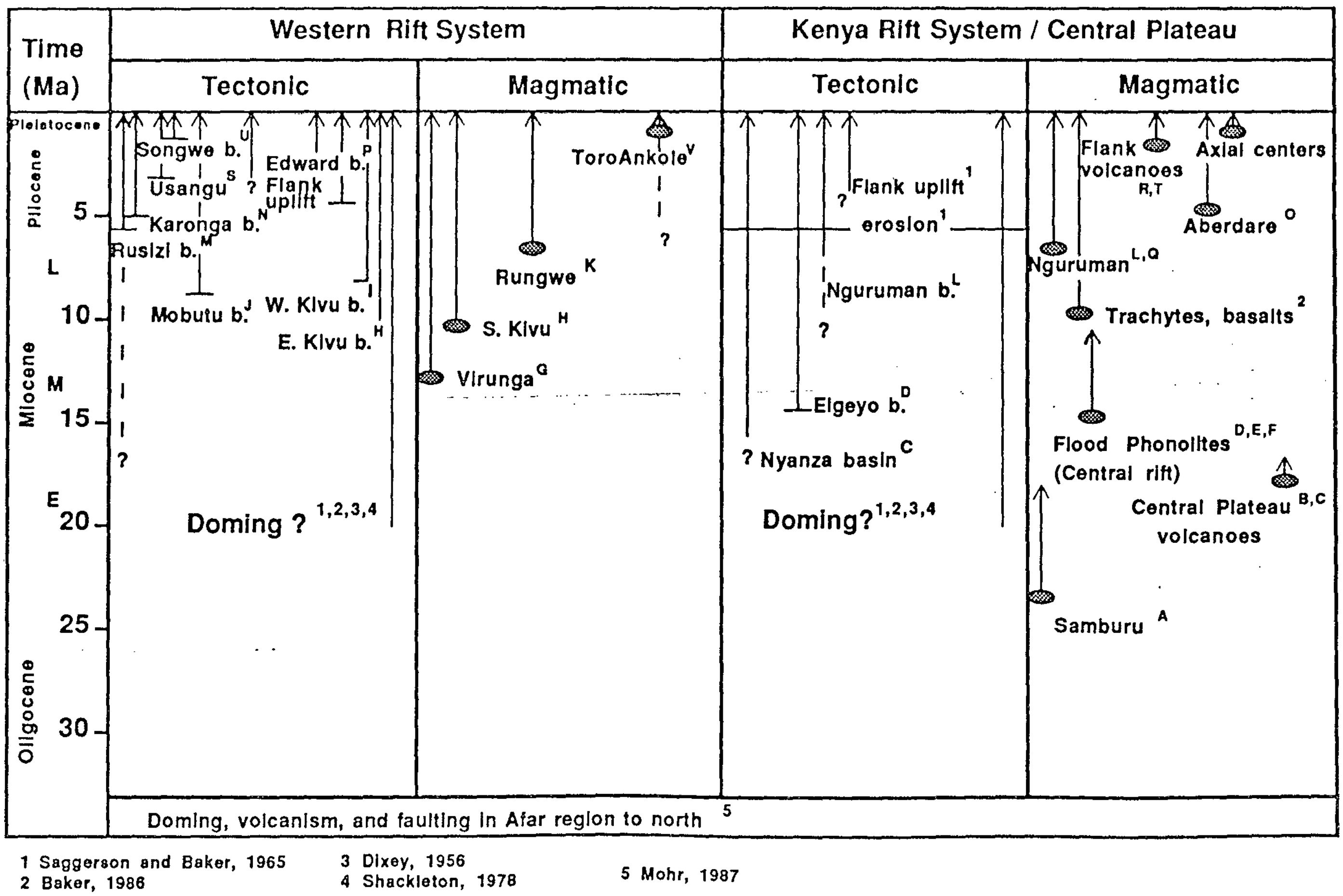

Figure 14. Chronologic constraints on vertical movements, volcanic activity, and basinal subsidence within the East African Plateau region. Lines indicate approximate time span of activity (dashed, ? where uncertain). Letters refer to timing constraints listed in Tables 1 and 2. Note lag between initial volcanism and development of sedimentary basins.

depth to detachments, and the rollover geometry of basins suggest that high-angle, planar border-fault systems along one side of Western rift basins extend to the base of the crust (for example, Zana and Hamaguchi, 1978; Shudofsky, 1985). In the case of full-graben morphologies, observations within the Kivu basin suggest that full-graben morphologies may be relict features; by mid-Pleistocene time, the West Kivu border-fault segment became the active border-fault segment, and only minor offsets occurred along the East Kivu border-fault segment (Ebinger, 1989). This shift may indicate a regional evolution to border-fault segments along the western side of the rift.

The geometrical relations noted above are not unique to the Western rift system, as similar patterns of alternating basinal asymmetries, border-fault segmentations, and geometries of border-fault linkage have been described within the Kenya rift system that has formed along the eastern side of the East African Plateau (King, 1978; Bosworth, 1985; Baker, 1986). Seismic data from the Kenya rift valley also indicate that little or no crustal thinning or magmatic intrusion has occurred beneath the uplifted rift flanks (Maguire and Long, 1976; Long and Backhouse, 1976; Bram and Schmeling, 1975; Hebert and Langston, 1985; Savage and Long, 1985).

TIMING OF CRUSTAL MOVEMENTS IN EAST AFRICA

To summarize timing constraints within the East African Plateau region, initial volcanic activity preceded or was concurrent with initial faulting, and this early Miocene volcanism occurred in isolated centers across the central part of the uplifted region prior to faulting and basinal subsidence in either the Kenya or Western rift systems (Fig. 14; Table 1). Volcanic activity in the northern and central Kenya rift commenced 11 m.y. prior to volcanic activity in the future Western rift system (Fig. 14). During the past 10 m.y., magmatic activity generally has been localized in the fault-bounded basins of the present-day Western rift where active volcanoes are located along faults and fissures parallel to border faults and along transfer faults crosscutting the rift valley. Similar patterns have been noted in the Kenya rift, although Pliocene-Recent volcanic centers (Kenya and Marsabit) are located along the eastern flanks of the Kenya rift (for example, Baker and others, 1971; King, 1978; Bosworth, 1987) (Fig. 14). Thus, owing to the 11-m.y.-longer history of volcanism within the Kenya rift, differences between the two rift systems largely can be interpreted as differences in the time span of volcanism and stage of development.

Because of the along-axis variations in elevation and lake level fluctuations in the Western rift valley, it is difficult to establish horizontal data for crustal movements during the development of individual basins (for example, Livingstone, 1965; Hecky and Degens, 1973; Ebinger and others, 1984; Johnson and others, 1987). Several indirect lines of evidence, however, indicate that uplift of the rift flanks superimposed on the plateau topography was concurrent with or postdated initial volcanism and faulting along the length of both the Western and Kenya rifts. The oldest known Western rift sequences are upper Miocene (~8 Ma); changes in drainage patterns across the plateau indicate that rift flank uplift was most rapid during late Pliocene–Pleistocene time (Bishop and Posnansky, 1960; Holmes, 1978; Grove, 1983; Baker, 1986; M. Pickford, 1989, personal commun.). During late Pliocene or Pleistocene time, rates of uplift along the northeastern flanks of the Western rift system exceeded rates of downcutting along several rivers that previously had flowed north into the Nile drainage basin, and rivers that originally flowed west into the Congo basin were diverted by uplift along the eastern flanks of the rift (Bishop and Posnansky, 1960; Holmes, 1978; Grove, 1983; Baker, 1986). These rivers are now ponded in shallow lakes in the central uplifted plateau between the Western and Kenya rift systems (Fig. 12). Late Pleistocene uplift along the eastern margin of the Kivu and northern Tanganyika rift basins produced eastward-tilted strand lines along the western margin of Lake Victoria (Bishop and Posnansky, 1960).

Uplifted terraces of lake sequences indicate that rift flank uplift has narrowed the initial zone of subsidence within basins (Table 1). For example, terraces of Pliocene-Pleistocene lacustrine sequences found along the central parts of border-fault segments were once contiguous with sequences found at 500- to 800-m-lower elevations (for example, East Kivu basin) and on the monoclinal side of basins (for example, Rusizi basin). The morphology of step faults along border-fault segments indicates that the innermost triangular fault scarp is active, as higher scarps are deeply dissected, and basin margins beneath the lake are steep (>40°). This narrowing of the basins with collapse of the hanging wall of border faults appears to be synchronous with uplift along both sides of rift basins. Both progressive collapse of the hanging wall and narrowing of basins with rift flank uplift are similar to spatial patterns predicted by geometric and thermo-mechanical models of planar detachments (for example, Gibbs, 1983; Buck and others, 1988). A similar narrowing of Kenya rift basins has been noted, and lateritized upper Pliocene–Pleistocene basalts found along uplifted flanks formed at much lower elevations than present day (King, 1978).

ALONG-AXIS SEGMENTATION

One proposed mechanism for the along-axis segmentation, along-axis shifts in basin asymmetry, and the orientation of normal and strike-slip faults in transfer fault zones is a reactivation of pre-existing crustal shear zones (for example, Dixey, 1956; McConnell, 1972; Villeneuve, 1978). In a regional sense, the general outline of the Western rift system generally avoids the perhaps more deeply rooted cratonic areas within the East African Plateau region, although several border faults cut Archean basement (for example, Figs. 6, 10, and 11). At a shorter-length scale, a comparison of individual border and transfer faults to pre-rift structures reveals a poor correlation (Figs. 6, 7, 10, and 11). Exceptions to this generalization are normal faults bounding the Songwe border-fault segment (BFS21) noted above. In most instances, faults extend across contacts between tectonic units (for example, Moba basin) or crosscut fold axes and shear zones in metamorphic basement (Brown, 1964; Hopwood, 1970; Haldemann, 1969; Crossley and Crow, 1980; Ebinger and others, 1987, 1989). In part of the Western rift where basement faults and metamorphic foliations have a predominant north-south trend, or subparallel to the regional orientation of the Western rift system, there is little evidence for recent faulting along Precambrian mylonites and faults. Perhaps the initial location of volcanic centers within the East African Plateau was controlled by pre-existing weaknesses within the continental lithosphere, but late Cenozoic volcanic centers rarely follow pre-rift faults. Thus, the along-axis segmentation of the Western rift and the strike of transfer faults linking *en echelon* border-fault segments generally represent the response of old, cold continental lithosphere to rifting processes.

A second mechanism is changing stress orientations during discrete episodes of rifting. Although the timing of faulting in many parts of the Western rift system is poorly constrained, volcanic centers aligned along faults subparallel to border-fault systems have been episodically active throughout the history of the Kivu and Karonga basins (Ebinger, 1989; Ebinger and others, 1989). Likewise, focal planes of historic earthquakes parallel Miocene escarpments (Shudofsky, 1985). The geometry of accommodation zones, however, may change as new border-fault segments and extensional basins develop.

Some authors have suggested that an along-axis propagation of rifting contributes to the segmentation of rift systems, both continental and oceanic (for example, Macdonald and Fox, 1983; Ebinger and others, 1984; Bosworth, 1985; Bonatti, 1985). If one considers the repetitive and interactive relationship between faulting and magmatic processes, existing constraints suggest that volcanism, and probably faulting, propagated on both a regional and local scale within the East African Plateau region. A regional north-south age progression in volcanic activity has been recognized in the Kenya rift, and a similar north-south propagation of rifting has been suggested, based on geomorphological evidence in the Western rift (Capart, 1949; Haldemann, 1969; Shackleton, 1978; Crossley and Crow, 1980; Williams and Chapman, 1986; Bosworth, 1987) (Table 1). Volcanic flows from the Rungwe province, the southernmost Western rift volcanic province, are approximately 3 m.y. older than flows in the northern part of the Western rift (Table 1), but additional age constraints are needed to evaluate this trend. Given the temporal development of propagating rift basins in East Africa, Pliocene-Holocene shield volcanoes along the flanks of the Kenya rift may mark an incipient zone of crustal extension related to a southward propagation of the Ethiopian rift valley.

At the 100-km length scale of border-fault segments, isolated Western rift border-fault segments have propagated to the north and south to link discrete segments. For example, the Karonga and Rukwa border-fault segments developed between 7 and 5 Ma, and the Songwe border-fault segment developed between 2 and 0.5 Ma to connect these isolated *en echelon* basins (Fig. 4) (Ebinger and others, 1989). A progressive lengthening and coalescence of basins was interpreted from a comparison of seismic stratigraphic sequences within Malawi lake basins (Ebinger, 1984). Thus, a diachronous development contributes to the along-axis segmentation of the Western rift valley border-fault system. Morley (1988b) has suggested that the central Kenya rift (Elgeyo basin) nucleated at ~16 Ma and that volcanism and faulting propagated to the north and south away from this magmatically active region (Fig. 14).

By analogy, an along-axis propagation model for the observed segmentation of the Western rift is supported by studies of oceanic rift segmentation. In the Western rift, the geometrical arrangement of border-fault segments and transfer faults is similar to morphologic patterns observed along propagating oceanic spreading centers and in theoretical models of fault propagation (for example, Aydin and Pollard, 1982; Sempère and MacDonald, 1986). Crack propagation models predict stress concentrations in zones of overlap between *en echelon* cracks, perhaps analogous to the comparatively high-strain accommodation zones found in the Western rift (for example, Figure 9, Pollard and Aydin, 1984; Ebinger and others, 1989). Further studies are needed, however, to extend the results of oceanic studies to the rheologically more complicated continental lithosphere beneath East Africa.

CONCLUSIONS

The discontinuous Western rift is bounded by a series of high-angle planar border faults along one side of approximately 100-km-long, spoon-shaped sedimentary basins. Depth-to-detachment estimates of >20 km, rollover basin geometries, and seismicity patterns indicate that planar, high-angle border faults may penetrate the crust, effectively fracturing the mechanical lithosphere. The spatial distribution of fault systems and volcanic centers indicates that crustal extension is restricted to 40- to 70-km-wide rift basins bounded by border-fault segments. Structural field observations and focal mechanism solutions support a regional east-west extension direction, and estimates of crustal extension are 2%–15%. Because roughly comparable amounts of extension (2–10 km) and throws (1–6 km) have occurred along border faults, oblique-slip transfer faults commonly link Western rift basins. Along the length of the Western rift, volcanic provinces coincide with comparatively high-strain accommodation zones, and individual eruptive centers coincide with high-angle transfer faults and the tips of border-fault segments.

Volcanic provinces within both the Western and Kenya rift systems are older in the north than in the south, although initial volcanic activity in the northern Western rift at ~12 Ma began 11 m.y. later than initial volcanism in the Kenya rift at ~23 Ma. Initial volcanic activity preceded or was concurrent with initial faulting and subsidence within Western rift basins. Much of the uplift along the flanks of basins that is superimposed on the East African Plateau postdates initial volcanism and basin subsidence in the Western rift. The poor correlation between the location and attitude of late Cenozoic border/transfer faults and pre-rift structures indicates that the along-axis segmentation is not inherited. Instead, Western rift basins have developed diachronously, and border-fault propagation contributes to the observed segmentation of the Western rift valley, which is similar to that of other continental rifts and propagating oceanic rift systems.

ACKNOWLEDGMENTS

Permission to conduct field research was granted by the Ministère de l'Energie, des Mines, et des Artisants, Rwanda; Département de l'Energie et des Mines, Burundi; UTAFITI (Tanzanian National Scientific Research Council); and Institut de la Recherche Scientifique (Zaïre). J. Nanyaro (University of Dar es Salaam), K. Theunissen and J. Klerkx (Musée Royal de l'Afrique Centrale), L. Tack (University of Bujumbura), A. Tesha, J. Knight, L. Willey, S. Townsend, P. Tilke, P. Eeckelers, and many Peace Corps volunteers provided invaluable assistance in field areas. Revisions suggested by L. Royden, K. Hodges, J. Peirce, E. Uchupi, C. Morley, and W. Bosworth greatly improved the text. I thank J. Klerkx, K. Theunissen, L. Tack, B. Rosendahl, and J. Peirce for use of unpublished information, and P. Williamson, A. Cohen, D. Livingstone, and D. Grove for helpful discussions. I gratefully acknowledge Mobil Oil Exploration Production for photographic reproduction of Thematic Mapper imagery, and Amoco Production for making available proprietary data used in basinal analyses. This project was funded by a National Science Foundation (NSF) Presidential Young Investigator Award granted to L. Royden; Geological Society of America Student Research Grant 3754-87; Sea Grant NA84-AA-D-00033, R/G-11; and NSF Grant EAR84-18120.

APPENDIX 1. LANDSAT IMAGERY

Landsat-5 Multi-Spectral Scanner (MSS) and Thematic Mapper (TM) images used in this study cover regions of 185 km by 185 km. Standard radiometric and geometric corrections were made at the EROS processing center, and images are displayed using a space-oblique Mercator projection that preserves length and angular relations. False-color composite images corresponding to scenes 1, 2, 3, and 4 were generated from reflectance data in bands 2 (0.5–0.6 μm), 4 (0.6–0.7 μm), and 5 (0.8–1.1 μm), displayed as blue, green, and red, respectively. Digital data from TM scene 5 (Fig. 1) were processed to enhance faults and lineaments and to distinguish volcanic units, using a variety of filtering, color-ratioing, and contrast-stretching techniques. MSS images 1–4 shown in Figure 1 are E-50870-07370, E-50143-07380, and E-50143-07382; TM image is Y-50850-07204. The quality of data is excellent; cloud cover was less than 20% in scene 2 and less than 10% in scenes 1, 3, 4, and 5.

REFERENCES CITED

Afonso, A., 1976, A geologia de Moçambique: Maputo, Mozambique, Dir. Serv. Geol. Minas, 142 p.

Arambourg, C., 1933, Les formations pré-tertiares de la bordure occidentale du lac Rodolphe (Afrique Orientale): Comptes Rendus de l'Académie des Science, Paris, v. 197, p. 1663–1665.

Aydin, A., and Pollard, D. D., 1982, Origins of the zig-zag pattern of normal faults: Geological Society of America Abstracts with Programs, p. 436.

Bagdasaryan, G. P., Gerasimovskiy, V. I., Polyakov, A. I., and Gukasyan, R. Kh., 1973, Age of volcanic rocks in the rift zones of East Africa: Geochemistry International, v. 1973, p. 66–71.

Baker, B. H., 1986, Tectonics and volcanism of the southern Kenya rift valley and its influence on rift sedimentation, *in* Frostick, L. E., and others, eds., Sedimentation in the East African rifts: Geological Society of London Special Publication 25, p. 45–57.

Baker, B. H., Williams, L.A.J., Miller, J. A., and Fitch, F. J., 1971, Sequence and geochronology of the Kenya rift volcanics: Tectonophysics, v. 11, p. 191–215.

Bally, W., 1982, Musings over sedimentary basin evolution: Royal Society of London Philosophical Transactions, v. A305, p. 325–328.

Bellon, H., and Pouclet, A., 1980, Datations K-Ar de quelques laves du Rift-ouest de l'Afrique Centrale: Implications sur l'évolution magmatique et structurale: Geologische Rundschau, v. 69, p. 49–62.

Bishop, W. W., and Posnansky, M., 1960, Pleistocene environments and early man in Uganda: Uganda Journal, v. 24, p. 44–61.

Bonatti, E., 1985, Punctiform initiation of seafloor spreading in the Red Sea during transition from a continental to an oceanic spreading center: Nature, v. 316, p. 33–37.

Bosworth, W., 1985, Geometry of propagating continental rifts: Nature, v. 316, p. 625-627.
——— 1987, Off-axis volcanism in the Gregory rift, East Africa: Implications for models of continental rifting: Geology, v. 15, p. 397-400.
Bram, K., and Schmeling, B. D., 1975, Structure of crust and upper mantle beneath the Western rift of East Africa, derived from investigations of near earthquakes, *in* Pilger, A., and Rosler, A., eds., Afar between continental and oceanic rifting: Stuttgart, Germany, Schweizerbart, p. 138-142.
Brock, P.W.G., 1962, Tundumu rift valley: University of Leeds Annual Report, 6th, p. 31.
Brown, C., and Girdler, R. W., 1980, Interpretation of East African gravity data and its implications for the breakup of the continents: Journal of Geophysical Research, v. 85, p. 6443-6455.
Brown, P., 1964, The Songwe scarp carbonatite and associated feldspathization in the Mbeya range, Tanganyika: Geological Society London Quarterly Journal, v. 120, p. 223-240.
Buck, W. R., Martinez, F., Steckler, M. S., and Cochran, J. R., 1988, Thermal consequences of lithospheric extension: Pure and simple: Tectonics, v. 7, p. 213-234.
Burchfiel, B. C., and Stewart, J., 1966, The "pull-apart" origin of Death Valley, California: Geological Society of America Bulletin, v. 77, p. 439-442.
Burgess, C., Rosendahl, B. R., Sander, S., Burgess, C. A., Lambiase, J., Derksen, S., and Meader, N., 1989, The structural and stratigraphic evolution of Lake Tanganyika: A case study of continental rifting, *in* The Triassic System of the eastern United States: American Association of Petroleum Geologists Special Publication (in press).
Cahen, L., and Snelling, I., 1984, The geochronology and evolution of Africa: Oxford, United Kingdom, Clarendon Press, 591 p.
Capart, A., 1949, Sondages et carte bathymétrique, *in* Exploration hydrobiologique du lac Tanganyika (1946-1947): Brussels, Belgium, Institut Royal des Sciences Naturelles Belge, p. 1-16.
Carter, G., and Bennett, J., 1973, The geology and mineral resources of Malawi: Geological Survey Department Malawi Bulletin, v. 6, 62 p.
Chorowicz, J., 1983, Le rift est-africain: Debut de l'ouverture d'un ocean?: Bulletin Centres Récherches Exploration-Production Elf-Aquitaine, v. 7, p. 155-162.
Chorowicz, J., and Thouin, C., 1985, Failles synsedimentaires et structure de la plaine de la Rusizi (Nord Tanganyika): Comptes Rendus de l'Académie des Sciences, Paris, v. 301, p. 835-841.
Coffin, M., and Rabinowitz, P., 1983, East African continental margin transect, *in* Bally, A. W., ed., Structural styles: American Association of Petroleum Geologists Studies in Geology 2, p. 2.3.3-22.
Combe, A. D., 1943, The geology of the southern part of Ruwenzori: Geological Survey Uganda Annual Report, 1943, p. 4-15.
Courtillot, V., Armijo, R., and Tapponnier, P., 1987, The Sinai triple junction revisited: Tectonophysics, v. 141, p. 181-190.
Crossley, R., and Crow, M. J., 1980, The Malawi rift, *in* Geodynamic evolution of the Afro-Arabian rift system: Rome, Italy, Accademia Nationale Lincei, p. 77-87.
Crossley, R., and Knight, R. M., 1981, Volcanism in the western part of the rift valley in southern Kenya: Bulletin of Volcanology, v. 44-2, p. 117-128.
Crough, S. T., 1983, The correction for sediment loading on the seafloor: Journal of Geophysical Research, v. 88, p. 6449-6454.
Daly, M. C., 1986, Crustal shear zones and thrust belts: Their geometry and continuity in Central Africa: Royal Society of London Philosophical Transactions, v. A317, p. 111-128.
Davies, K. A., 1951, The Uganda section of the Western rift: Geology Magazine, v. 88, p. 377-385.
Degens, E. T., Von Herzen, R. P., and Wong, H. K., 1971, Lake Tanganyika: Water chemistry, sediments, and geological structure: Naturwissenschaften, v. 58, p. 229-241.
Degens, E. T., Von Herzen, R. P., Wong, H. K., Deuser, W. G., and Jannasch, H. W., 1973, Lake Kivu: Structure, chemistry, and biology of an East African rift lake: Geologische Rundschau, v. 62, p. 245-277.
de la Vallée Poussin, M., 1933, Quelques faits nouveaux apropos du graben central africain: Bulletin Société Belge Géologique, v. 43.
De Mulder, M., and Pasteels, P., 1986, K-Ar geochronology of the Karisimbi volcano (Virunga, Rwanda-Zaïre): Journal of African Earth Sciences, v. 5, p. 575-579.
Dixey, F., 1956, The East African rift system: Colonial Geological Mineral Resources, no. 1.
Drake, R. E., Van Couvering, J. A., Pickford, M. H., Curtis, G. H., and Harris, J. A., 1988, New chronology for the early Miocene mammalian faunas of Kisingiri, western Kenya: Geological Society of London Journal, v. 145, p. 479-491.
Ebinger, C. J., 1989, Geometry and kinematics of border faults and accommodation zones, Kivu-Rusizi rift, Africa: Tectonics, v. 8, p. 117-133.
Ebinger, C. J., Crow, M. J., Rosendahl, B. R., Livingstone, D. L., and LeFournier, J., 1984, Structural evolution of Lake Malawi, Africa: Nature, v. 308, p. 627-629.
Ebinger, C., Rosendahl, B., and Reynolds, D., 1987, Tectonic model of the Malawi rift, Africa, *in* Ben-Avraham, Z., ed., Sedimentary basins within the Dead Sea and other rift zones: Tectonophysics, v. 141, p. 215-235.
Ebinger, C. J., Bechtel, T. D., Forsyth, D. W., and Bowin, C. O., 1989, Effective elastic plate thickness beneath the East African and Afar plateaux and dynamic compensation for the uplifts: Journal of Geophysical Research (in press).
Ebinger, C., Deino, A., and Drake, B., 1989, Chronology of volcanism and rift basin propagation: Rungwe volcanic province, East Africa: Leeman, W., and Fitton, G., eds., Magmatism and lithospheric extension: Journal of Geophysical Research (in press).
Fairhead, J., and Girdler, R. W., 1969, How far does the rift system extend through Africa?: Nature, v. 221, p. 1018-1020.
Fairhead, J., and Stuart, G., 1982, The seismicity of the East African rift system and comparison with other continental rifts, *in* Pálmason, G., ed., Continental and oceanic rifts: Washington, D.C., American Geophysical Union, p. 41-61.
Fick, L. J., and Van der Heyde, C., 1959, Additional data on the geology of the Mbeya carbonatite: Economic Geology, v. 54, p. 842-872.
Gibbs, A. D., 1983, Balanced cross-section construction from seismic sections in areas of extensional tectonics: Journal of Structural Geology, v. 5, p. 153-160.
——— 1984, Structural evolution of extensional basin margins: Geological Society of London Journal, v. 141, p. 609-620.
Grantham, D. R., Teale, E. O., Spurr, A. M., Harkin, D. A., and Brown, P. E., 1958, Quarter degree sheet 224 (Mbeya): Geological Survey Tanganyika.
Gregory, J., 1896, The Great Rift Valley: London, United Kingdom, John Murray, 405 p.
Grove, A. T., 1983, Evolution of the physical geography of the East African rift valley region, *in* Sims, R. W., Price, J. H., and Whalley, P.E.S., eds., Evolution, time, and space: The emergence of the biosphere: London, United Kingdom, Academic Press, p. 115-155.
Guibert, Ph., 1977, Contribution a l'étude du volcanisme du Sud-Kivu (Zaïre): I: La chaîne volcanique Tshibinda-Kalehe: Archive Science Genève, v. 30, p. 15-27.
Haldemann, E. G., 1969, Geological and physiographical setting of the Kalambo Falls prehistoric site, *in* Clark, J. D., ed., Kalambo Falls prehistoric site: Cambridge, United Kingdom, Cambridge University Press, p. 20-45.
Harkin, D. A., 1960, The Rungwe volcanics at the northern end of Lake Nyasa: Geological Survey Tanganyika Memoir II, 172 p.
Harkin, D. A., and Harpum, J. R., 1978, Quarter degree sheet 78 (Tukuyu): Geological Survey Tanganyika.
Hebert, L., and Langston, C., 1985, Crustal thickness estimate at AAE (Addis-Ababa, Ethiopia) and NAI (Nairobi, Kenya) using teleseismic P-wave conversions: Tectonophysics, v. 111, p. 299-327.
Hecky, R. E., and Degens, E. T., 1973, Late Pleistocene-Holocene chemical stratigraphy and paleolimnology of the rift valley lakes of central Africa: Woods Hole Oceanographic Institution Technical Report WHOI 73-28, 93 p.
Holmes, A., 1951, Evidence of lava formation *in situ*, south-west Uganda: Geological Magazine, v. 88, p. 73-87.
——— 1978, Holmes principles of physical geology: New York, John Wiley & Sons, p. 647-657.
Hopwood, A. M., 1970, Structural reorientation as evidence of basement warping associated with rift faulting in Uganda: Geological Society of America Bulletin, v. 81, p. 3473-3480.
Hopwood, A., and Lepersonne, J., 1953, Présence de formations d'age miocene inferieur dans le fossé tèctonique du lac Albert: Annals Société Géologique Belge, v. 77, p. 83-113.
Ilunga, L. K., 1984, Le quaternaire de la plaine de la Ruzizi [Ph.D. dissert.]: Bruxelles, Belgium, University Bruxelles, 340 p.
Johnson, T. C., Halfman, J. D., Rosendahl, B. R., and Lister, G. S., 1987, Climatic and tectonic effects on sedimentation in a rift valley lake: Evidence from high-resolution seismic profiles, Lake Turkana, Kenya: Geological Society of America Bulletin, v. 98, p. 439-447.
Kampunzu, A. B., Vellutini, P.-J., Caron, J.-P., Luahala, R. T., Kanika, M., and Rumvegeri, B. T., 1983, Le volcanisme et l'évolution structurale du Sud-Kivu (Zaïre): Bulletin Centres Récherches Exploration-Production Elf-Aquitaine, v. 7, p. 257-271.
Kaufulu, Z., Vrba, E., and White, T., 1981, Age of the Chiwondo beds, northern Malawi: Annals of the Transvaal Museum, v. 33, p. 1-8.
Kent, P. E., Hunt, J. A., and Johnstone, D. W., 1971, The geology and geophysics of coastal Tanzania: Institute for Geological Sciences, Geophysical Paper 6, 101 p.
King, B. C., 1978, Structural and volcanic evolution of the Gregory rift valley, *in* Bishop, W. W., ed., Geologic background to fossil man: Edinburgh, Scotland, Scottish Academic Press, p. 29-54.
Klerkx, J., and Nanyaro, J. T., 1988, The Ukinga Group in southwestern Tanzania: A shear belt of Middle Proterozoic age?: IGCP Newsletter 255, v. 1, p.37-41.
Kenya Rift International Scientific Project, 1987, Working Group, Kenya Rift International Scientific Project: Preliminary results: Nature, v. 325, p. 239-242.
Lavreau, J., Patricec, V., and Waleffe, A., 1981, Carte lithologique du Rwanda (1:250,000): Tervuren, Belgium, Musée Royal de l'Afrique Centrale.
Lepersonne, J., 1977, Carte géologique du Zaïre (1:2,000,000): Tervuren, Belgium, Musée Royal de l'Afrique Centrale.
Livingstone, D. A., 1965, Sedimentation and the history of water level change in Lake Tanganyika: Limnology and Oceanography, v. 10, p. 607-610.
Long, R., and Backhouse, R., 1976, The structure of the western flank of the Gregory rift (Kenya), Part II: The mantle: Royal Astronomical Society Geophysical Journal, v. 44, p. 677-688.
Lorber, P. M., 1984, The Kigoma basin of Lake Tanganyika: Acoustic stratigraphy and structure of an active continental rift [M.S. thesis]: Durham, North Carolina, Duke University, 76 p.
Macdonald, K. C., and Fox, P. J., 1983, Overlapping spreading centers: A new kind of accretionary plate boundary on the East Pacific Rise: Nature, v. 302, p. 55-58.
Maguire, P., and Long, R., 1976, The structure of the western flank of the Gregory rift (Kenya), Part I: The crust: Royal Astronomical Society Geophysical Journal, v. 44, p. 661-675.
McConnell, R. B., 1950, Outline of the geology of Ufipa and Ubende: Geological Survey Tanganyika Bulletin, v. 19, 60 p.
——— 1972, Geological development of the rift system of eastern Africa: Geological Society of America Bulletin, v. 83, p. 2549-2572.
Mohr, P. A., 1987, Structural style of continental rifting in Ethiopia: Reverse décollements: EOS (American Geophysical Union Transactions), v. 68, p. 721-729.
Morley, C. K., 1988a, Variable extension in Lake Tanganyika: Tectonics, v. 7, p. 785-801.
——— 1988b, Comment on "Off-axis volcanism in the Gregory rift, East Africa: Implications for models of continental rifting": Geology, v. 16, p. 569.
Pasteels, P., De Paepe, P., Villeneuve, M., and Klerkx, J., 1989, Age of the volcanism of the southern Kivu area (Western rift: Burundi, Rwanda, Zaire): Earth and Planetary Science Letters (in press).
Patterson, M. B., 1983, Structure and acoustic stratigraphy of the Lake Tanganyika rift valley [M.S. thesis]: Durham, North Carolina, Duke University, 89 p.
Peirce, J., and Lipkov, L., 1988, Structural interpretation of the Rukwa rift, Tanzania: Geophysics, v. 53, p. 824-836.
Pickford, M., 1987, Implications of the Albertine (Uganda) fossil mollusc sequence: Comptes Rendus de l'Académie des Sciences, Paris, v. 305, p. 317-322.
Pollard, D. D., and Aydin, A., 1984, Propagation and linkage of oceanic ridge segments: Journal of Geophysical Research, v. 89, p. 10,017-10,028.
Pouclet, A., 1975, Histoire des grands lacs de l'Afrique centrale: Mise au point des connaissances actuelles: Revues Géographie Physique Géologie Dynamique, v. 17, p. 475-482.
——— 1977, Contribution a l'étude structurale de l'aïre volcanique des Virunga, rift de l'Afrique centrale: Revues Géographie Physique et Géologie Dynamique, v. 19, p. 115-124.
Quennell, A. M., McKinlay, A.C.M., and Aitken, W. G., 1956, Summary of the geology of Tanganyika: Geological Survey Tanganyika Memoirs, 264 p.
Reeves, W., 1960, Geologic map of Northern Rhodesia (1:1,000,000); Geological Survey Department Rhodesia.
Rodrigues, E. B., 1970, Seismological studies of the East African rift system [Ph.D. dissert.]: Nairobi, Kenya, University of East Africa, 187 p.
Rosendahl, B., Reynolds, D., Lorber, P., Scott, D., McGill, J., and Lambiase, J., 1986, *in* Frostick, L. E., and others, eds., Sedimentation in the East African rifts: Geological Society of London Special Publication 25, p. 29-34.
Rykounov, L. N., Sedov, V. V., Savrina, L. A., and Bourmin, V. J., 1972, Study of microearthquakes in the rift zones of East Africa, *in* Girdler, R. W., ed., East African rifts: Tectonophysics, v. 15, p. 123-130.
Saggerson, E. P., and Baker, B. H., 1965, Post-Jurassic erosion surfaces in eastern Kenya and their deformation in relation to rift structure: Geological Society of London Quarterly Journal, v. 121, p. 5-72.
Savage, J.E.G., and Long, R. E., 1985, Lithospheric structure beneath the Kenya Dome: Royal Astronomical Society Geophysical Journal, v. 82, p. 461-477.
Sempère, J.-C., and MacDonald, K., 1986, Overlapping spreading centers: Implications from crack growth simulation by displacement continuity method: Tectonics, v. 5, p. 151-163.
Shackleton, R. M., 1978, Structural development of the East African rift system, *in* Bishop, W. W., ed., Geologic background to fossil man: Edinburgh, Scotland, Scottish Academic Press, p. 20-28.
Shudofsky, G. N., 1985, Source mechanisms and focal depths of East African earthquakes using Rayleigh wave dispersion and body-wave modelling: Royal Astronomical Society Geophysical Journal, v. 83, p. 563-614.
Spence, J., 1954, The geology of the Galula Coalfield, Mbeya district: Geological Survey Tanganyika, v. 25, 34 p.
Stockley, G., 1948, Geology of north, west, and central Njombe district, southern highlands province: Geological Survey Department Tanganyika, 68 p.
Tack, L., and DePaepe, P., 1983, Le volcanisme du Sud-Kivu dans le nord de la plaine de la Rusizi au Burundi et ses rélations avec les formations géologiques avoisinantes: Rapp. Ann Dept. Min. Geol. Mus. Roy. Afri. Centr., v. 1981-1982, p. 137-145.
Teale, E. O., Eades, N. W., Harkin, D. A., Harpum, J. R., and Horne, R. G., 1962, Quarter degree sheet 245 (Irambo): Geological Survey Department Tanganyika.
Theunissen, K., 1986, Carte géologique de Burundi, Feuille Rumonge: Burundi, Ministère Travaux Publiques Energie Mines.
——— 1989a, Carte géologique de Burundi, Feuille Cibitoke: Burundi, Ministère Travaux Publiques Energie Mines, Burundi (in press).
——— 1989b, Carte géologique du Burundi, Feuille Bujumbura: Burundi, Ministère Travaux Publiques Energie Mines, Burundi (in press).
Tiercelin, J. J., Chorowicz, J., Bellon, H., Richert, J.-P., Mwanbene, J. T., and Walgenwitz, F., 1988, East African rift system: Offset, age, and tectonic significance of the Tanganyika-Rukwa-Malawi intracontinental transcurrent fault zone: Tectonophysics, v. 148, p. 241-252.
Tshimanga, K., and Kabengele, M., 1981, Quelques données structurales sur la region des Marungu, Shaba (Zaire): Cahiers Géologiques University Paris, v. 98, p. 456-463.
Villeneuve, M., 1983, Les sillons tectoniques du precambrien superieur dans l'est du Zaïre: Comparaisons avec les directions du rift est-africain: Bulletin Centres Récherches Exploration-Production Elf-Aquitaine, v. 7, p. 163-174.
Wayland, E. J., 1934, Peneplains and some other erosional platforms: Geological Survey Uganda, Annual Report 1933, p. 77-79.
Weissel, J., Karner, G., and Cowie, P., 1987, On the cause of rift flank uplift: Forward modeling of topography and gravity anomalies over oceanic rifts: EOS (American Geophysical Union Transactions), v. 68, p. 411.
Wernicke, B., 1985, Uniform-sense normal simple shear of the continental lithosphere: Canadian Journal of Earth Sciences, v. 22, p. 108-125.
Williams, L.A.J., and Chapman, G. R., 1986, Relationships between major structures, salic volcanism and sedimentation in the Kenya rift from the equator north to Lake Turkana, *in* Frostick, L. E., and others, eds., Sedimentation in the East African rifts: Geological Society of London Special Publication 25, p. 59-74.
Williamson, P., and Savage, R. J., 1986, Early rift sedimentation in the Turkana basin, northern Kenya, *in* Frostick, L. E., and others, eds., Sedimentation in the East African rifts: Geological Society of London Special Publication 25, p. 267-284.
Wohlenberg, J., 1968, Seismizitat der ostafrikanischen Grabenzonen zwischen 4°N und 2°S sowie 23°E und 40°E: Veroffentlichung Bayerischen Kommission Internationale Erdmessung, v. 43, 95 p.
Wong, H.-K., and Von Herzen, R. P., 1974, A geophysical study of Lake Kivu, East Africa: Royal Astronomical Society Geophysical Journal, v. 37, p. 371-389.
Zana, N., and Hamaguchi, N., 1978, Some characteristics of aftershock sequences in the Western rift valley of Africa: Tôhoku University Scientific Reports, v. 5, p. 55-72.

Manuscript Received by the Society June 20, 1988
Revised Manuscript Received December 8, 1988
Manuscript Accepted December 15, 1988